How Do Tropical Sea Surface Temperatures Influence the Seasonal Distribution of Precipitation in the Equatorial Amazon?

RONG FU, ROBERT E. DICKINSON, MINGXUAN CHEN, AND HUI WANG

School of Earth and Atmospheric Sciences, Georgia Institute of Technology, Atlanta, Georgia

(Manuscript received 24 November 1999, in final form 4 April 2001)

ABSTRACT

Although the correlation between precipitation over tropical South America and sea surface temperatures (SSTs) over the Pacific and Atlantic has been documented since the early twentieth century, the impact of each ocean on the timing and intensity of the wet season over tropical South America and the underlying mechanisms have remained unclear. Numerical experiments have been conducted using the National Center for Atmospheric Research Community Climate Model Version 3 to explore these impacts. The results suggest the following.

1) Seasonality of SSTs in the tropical Pacific and Atlantic has an important influence on precipitation in the eastern Amazon during the equinox seasons. The eastern side of the Amazon is influenced both by the direct thermal circulation of the Atlantic intertropical convergence zone (ITCZ) and by Rossby waves. These processes are enhanced by the seasonal cycles of SSTs in the tropical Atlantic and Pacific. SSTs affect Amazon precipitation much less during the solstice seasons and in the western Amazon.
2) The seasonality of SSTs in the Atlantic more strongly affects Amazon rainfall than does that of the Pacific. Without the former, austral spring in the eastern equatorial Amazon would be a wet season, rather than the observed dry season. As a consequence of the lag at that time of the southward seasonal migration of the Atlantic SSTs behind that of the insolation, the Atlantic ITCZ centers itself near 10°N, instead of at the equator, imposing subsidence and low-level anticyclonic flow over the eastern equatorial Amazon, thus drying the air above the planetary boundary layer and reducing the low-level moisture convergence. Consequently, convection in the eastern Amazon is suppressed despite strong surface heating.
3) Seasonality of the SSTs in the tropical Pacific also tends to reduce precipitation in the eastern Amazon during both spring and fall. In spring, subsidence is enhanced not only through a zonal direct circulation, but also through Rossby waves propagating from the extratropical South Pacific to subtropical South America. This teleconnection strengthens the South Atlantic convergence zone (SACZ) and the Nordeste low, in both cases reducing precipitation in the eastern Amazon. A direct thermal response to the Pacific SSTs enhances lower-level divergence and reduces precipitation from the northern tropical Atlantic to the northeastern Amazon.

1. Introduction

The wet season of the equatorial Amazon persists from austral spring to fall near the Andes, but near the Atlantic Ocean it is much shorter, peaking in austral fall (see Fig. 1, and, e.g., Henry 1922; Salati et al. 1979; Figueroa and Nobre 1990; Fu et al. 1999; Marengo et al. 2001). Hence, the eastern Amazon has just enough rainfall to maintain the growth of its vegetation. A delayed onset or earlier ending of the wet season would impose significant stress on the rainforest and agriculture (Nepstad et al. 1999). In addition to such local impacts, precipitation in the Amazon may influence many aspects of the seasonal pattern of atmospheric circulation in the North Atlantic (Namias 1972) and the establishment of the Bolivian high (Lenters and Cook 1997) farther south. Hence, the seasonal cycle must be understood in detail for successful modeling and prediction of variations of climate over tropical and subtropical South America.

Both continental surface heating (i.e., Gutman and Schwedtfeger 1965; Rao and Erdogan 1989; Lenters and Cook 1995) and sea surface temperatures (SSTs) in the tropical Atlantic and Pacific (e.g., Hastenrath and Heller 1977; Aceituno 1988; Enfield 1996; Nobre and Shukla 1996) can affect the seasonality of Amazon rainfall. However, how much these two factors contribute to the distribution and variation of the Amazon rainfall has previously been unclear and even controversial. For example, whether the moisture for precipitation is transported from the ocean or derived from land evapotranspiration has been debated. River chemical analysis (Gibbs 1979) and also water budget studies (e.g., Brubaker et al. 1993) support the hypothesis that the water vapor transported from the Atlantic Ocean provides much of the Amazon rainfall. The contrary view that

Corresponding author address: Dr. Rong Fu, Earth and Atmospheric Sciences, Georgia Institute of Technology, 221 Bobby Dodd Way, Atlanta, GA 30332-0340.
E-mail: fu@eas.gatech.edu

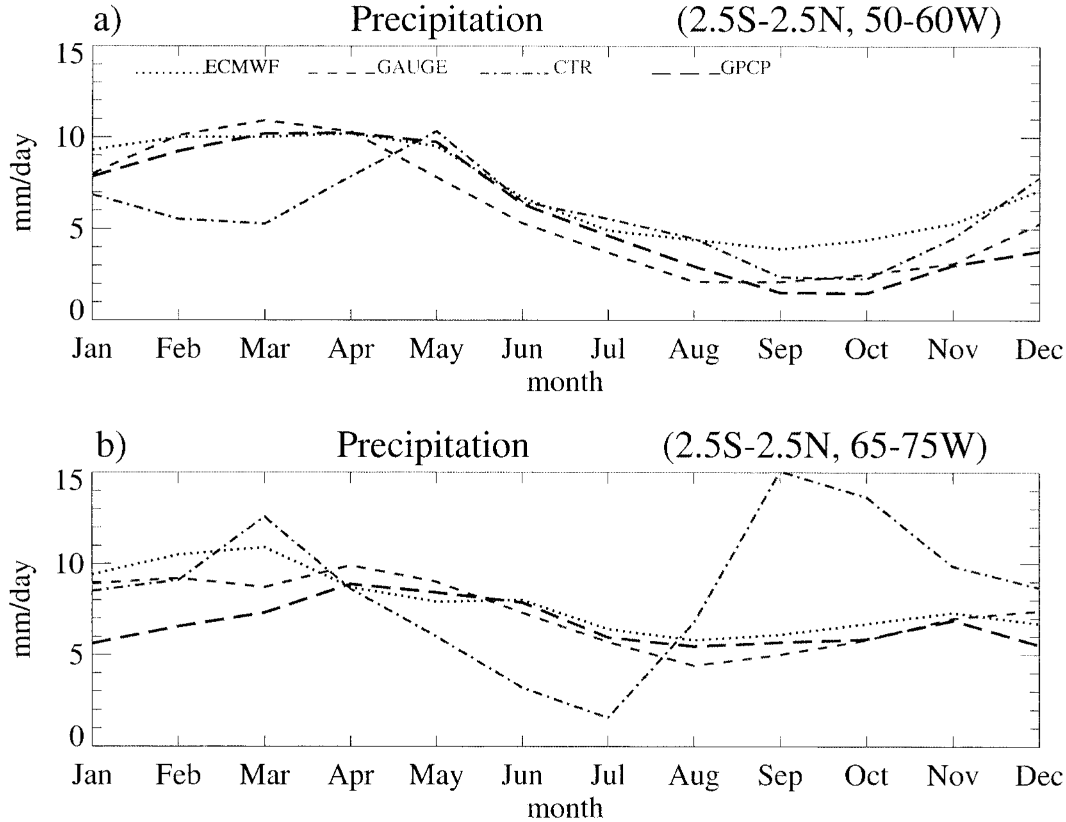

FIG. 1. (a) Monthly averaged precipitation (mm day^{-1}) over the equatorial eastern Amazon (2.5°S–2.5°N, 50°–60°W) derived from GPCP (long-dashed curve), rain gauge network (dashed curve), ECMWF reanalyses (dotted curve), and CCM3 control experiment (dot–dashed curve). (b) As in (a) but for the western equatorial Amazon (2.5°S–2.5°N, 65°–75°W).

much of the Amazon rainfall is from local recycling of water is supported by isotopic analyses (Salati et al. 1979). The relative importance of ocean and land to Amazon rainfall may vary in different parts of the Amazon. Rainfall in the areas from northeast Brazil to the central Amazon has been shown to correlate with the El Niño–Southern Oscillation (ENSO; Aceituno 1988) and the distribution of SSTs in the tropical Atlantic (Hasternrath and Heller 1977). However, correlation between rainfall in the western equatorial Amazon and SSTs is weak or nonexistent (Enfield 1996).

Moura and Shukla (1981) showed that a direct thermal circulation driven by warm SST anomalies in the Atlantic intertropical convergence zone (ITCZ) descends to the south of the heating source, and generates a low-level anticyclonic flow to the southwest. Hence, warm SST anomalies at 10°N in the Atlantic Ocean lead to droughts in northeast Brazil. However, whether or not the same mechanism can suppress rainfall in the eastern Amazon during austral spring when the land surface solar heating reaches its semiannual peak has not been previously addressed.

The effects of ENSO on Amazon rainfall have been well established by empirical studies of climate records but not the underlying mechanisms. The distinction between the direct effects of El Niño and those imposed through Atlantic SST anomalies has not been clearly established. For example, although the interannual variations of precipitation in northeast Brazil correlate with ENSO, this apparent influence of ENSO on Amazon rainfall may actually be caused by changes in moisture transport from the Atlantic Ocean that correlate to ENSO (Marengo 1992; Rao et al. 1996). Since SSTs in the tropical Atlantic are influenced by their own variability (Weare 1977; Zebiak 1993; Nobre and Shukla 1996) and by ENSO (Lau and Nath 1994; Saravanan and Chang 2000), whether or not moisture transport from Atlantic Ocean would change with ENSO if Atlantic SSTs were unchanged has not been clarified. Earlier numerical experiments have shown that the Amazon rainfall can be reduced by heating anomalies in either the eastern or western Pacific (Buchmann et al. 1989; Gandu and Silva Dias 1998). But how rainfall can be reduced by these remote influences has been unclear. Answers to this question would help to determine the mechanisms that control the teleconnection between ENSO and droughts in northeastern Brazil.

This work explores the sensitivity of the Amazon rainfall to changes of SSTs in the adjacent oceans and clarifies the roles of the tropical Pacific and Atlantic in determining the seasonal patterns of precipitation in the equatorial Amazon. This is the first step toward understanding the relative contribution of the remote oceanic influences versus the regional land surface conditions to the precipitation climatology in the Amazon basin. We will examine the following questions.

1) How important is the seasonality of the SSTs in the adjacent oceans for determining the seasonality of the Amazon rainfall compared to that of the land surface heating?
2) What role does the seasonality of SSTs in the tropical Atlantic play in shaping the seasonal pattern of precipitation in the eastern Amazon? What causes the dryness in austral spring in the equatorial eastern Amazon?
3) How does the seasonality of SSTs in the tropical Pacific influence the Amazon rainfall? Can Pacific SST anomalies change the low-level moisture transport from the Atlantic Ocean to the Amazon even with Atlantic SSTs remaining unchanged?

To isolate the influences of seasonal cycles of SSTs in each ocean, we conduct experiments in which SSTs vary seasonally in only one of the tropical oceans. The magnitudes of our hypothetical changes in surface forcing among these experiments are considerably larger than are the interannual changes in nature and thus more likely to produce interpretable responses in a climate model. Through analyzing the results of the experiments, we hope to establish the physical links between the seasonal cycles of SSTs in each ocean and the changes of the local atmospheric instability and hence precipitation. Our intention is to qualitatively determine how seasonal migration of the Pacific and Atlantic SSTs, respectively, influence the seasonality of the Amazon rainfall. Although the results cannot be directly applied to observed interannual variations of the Amazon rainfall, they clarify many aspects including what processes may contribute to a weakening of the wet season, and hence drought conditions (Liebmann and Marengo 2001).

2. Datasets and models

The geographical and seasonal patterns of precipitation and associated meteorological conditions in the Amazon region are derived from the Global Precipitation Climatology Project (GPCP) blended precipitation data (Huffman et al. 1997), and independently from more than 200 rain gauges over the Brazilian Amazon (including many that were not used in the blended data). Operational radiosonde profiles provide the vertical temperature, humidity, and wind structures at Manaus (3°S, 60°W) and Belém, Brazil (1.5°S, 49°W), and the European Centre for Medium-Range Weather Forecasts (ECMWF) reanalyses provide fields that are not available observationally.

The monthly precipitation distributions from the GPCP dataset are for the period of July 1987 through December 1993. They were derived by incorporating low-orbit microwave data from Special Sensor Microwave/Imager from the Defense Meteorological Satellite Program, infrared radiances from a set of high-orbit geostationary satellites, and rain gauge measurements. This merging technique infers spatial patterns of precipitation from the satellite observations and calibrates them according to ''ground truth'' provided by rain gauge measurements. Over land where surface microwave emission is heterogeneous, measurements at the 85-GHz frequency were combined with infrared radiances to provide the satellite estimate of precipitation. Warm rain, such as that produced by topographically forced cumulus convection, is likely to be underestimated since the infrared threshold technique can only detect high/cold clouds and the microwave scattering is mainly contributed by ice hydrometeors. Hence, the observed Amazon precipitation may have residual biases because rain gauges are limited and unevenly distributed in space.

The National Centers for Environmental Prediction–National Center for Atmosphere Research (NCEP–NCAR) radiosonde global dataset provides profiles of geopotential height, temperature, dewpoint, and horizontal wind at more than 2000 upper-air stations (Gaffen 1996). Soundings from the Manaus and Belém upper-air stations, where measurements were available for at least 15 days month^{-1} through the period of 1987–93, are used to represent the atmospheric thermodynamic structure in the central and eastern equatorial Amazon region.

Four experiments have been performed using the NCAR Community Climate Model Version 3 (CCM3) coupled with the Biosphere–Atmosphere Transfer Scheme (CCM3–BATS; Kiehl et al. 1998; Dickinson et al. 1993) to determine how seasonal changes of SSTs in the adjacent oceans may affect the seasonal patterns of the precipitation over the equatorial Amazon. The control (CTR) run is forced by the observed climatological seasonal cycle of SSTs at the T42 resolution of the atmospheric model (about 2.8°), as provided by the Atmosphere Model Intercomparison Project for 1979–93 (Gates 1992), which averaged observations to a climatological seasonal cycle consisting of 12 calendar months. After a 1-yr spinup, we run the experiment for 10 yr forced by the same seasonal cycle of SSTs, and obtain a control climatology by averaging over the 10-yr model simulation. These results are used to assess the adequacy of the CCM3–BATS in simulating the seasonal changes of precipitation over the equatorial Amazon.

The Atlantic SST (ATL) experiment is designed to isolate the effect of the seasonal cycle of SSTs in the tropical Atlantic on precipitation over the tropical Amazon. SSTs vary seasonally only in the tropical Atlantic (30°S–30°N). All other oceanic areas are fixed to the observed annual means, which are the averages of monthly climatological values of 12 calendar months. A discontinuity at 30°N/S is avoided by gradually reducing the seasonal deviations to their annual means from 30° to 60° latitudes within the Atlantic Ocean using the following formula:

$$\mathrm{SST}(\alpha, \varphi) = \mathrm{SST}_{\mathrm{ann}}(\alpha, \varphi) + C(\varphi)\delta_s \mathrm{SST}(\alpha, \varphi), \quad (1)$$

where α and φ denote longitude and latitude, respectively, $\mathrm{SST}_{\mathrm{ann}}$ the annual mean SST at a map cell centered at (α, φ), and δ_sSST the seasonal departure of SST from its annual mean value for that cell. Here C is a coefficient defined as the following:

$$\begin{aligned}
&C = 0 \qquad \varphi \subset (-90°, -60°] \quad \text{and} \quad \varphi \subset [60°, 90°),\\
&C(\varphi) = (60° - |\varphi|)/30°\\
&\qquad\qquad \varphi \subset (-60°, -30°) \quad \text{and} \quad \varphi \subset (30°, 60°)\\
&C = 1 \qquad \varphi \subset [-30°, 30°] \qquad\qquad (2)
\end{aligned}$$

where φ is negative south of the equator and α starts from the Greenwich meridian and increases eastward.

The Pacific SST experiment (PAC) only allows SSTs to vary seasonally over the tropical Pacific in order to isolate the influence of the Pacific on precipitation over the Amazon. The annual mean SST simulation (ANN) assumes all SSTs are fixed to their annual means globally. A comparison between the two seasonally varying SST experiments (ATL and PAC) and the fixed SST run (ANN) indicates the influence of the SSTs in each of the tropical oceans on the seasonal cycle of rainfall in the Amazon.

A steady-state barotropical model is used to assess the remote atmospheric response to a tropical heating source in the upper level. The model consists of a steady barotropic vorticity equation linearized about a climatological mean state (e.g., Ting 1996) and applied at 200 mb. The solution is obtained by a conjugate-gradient method (Navon and Legler 1987) with a specified basic state and an anomalous divergence field, which is defined as the forcing of the barotropic model induced by diabatic heating. The horizontal shift of stationary Rossby wave energy is also examined using the stationary wave activity flux (Karoly et al. 1989).

3. Evaluation of the CCM3–BATS control run

The adequacy of CCM3 for testing the influence of SSTs on the Amazon rainfall is evaluated by comparing for dry and wet seasons the patterns of precipitation, vertical temperature, humidity and wind profiles, and upper-level streamfunction to the GPCP precipitation data, rain gauges, 6-yr-averaged radiosonde profiles at Manaus and Belém, and ECMWF reanalyses. Current atmospheric general circulation models, such as CCM3, cannot exactly reproduce observed conditions in the Amazon. The CTR run is forced by the climatological seasonal cycle of SSTs averaged from observations for the period of December 1978–September 1993. Therefore, its output may not be comparable to any particular year during this period. Hence, we only examine the basic climatological characteristics of the simulation related to precipitation, not whether a detailed agreement is achieved, in order to evaluate how adequate CCM3 may be for simulating the response to the seasonal changes of large-scale surface temperature gradient.

The seasonal cycles of the precipitation in the equatorial Amazon given by the CTR run are examined in Fig. 1. The simulated wet season in the eastern equatorial Amazon in austral fall is very similar to that observed (Fig. 1a), but the amount of rainfall is underestimated in February and March by 40%. The modeled wet season in the western Amazon occurs from austral spring to fall, also corresponding to that observed (Fig. 1b). However, the wet season is more pronounced and starts two months earlier in the austral spring than observed. The modeled peak precipitation amounts are greater than observed, being overestimated by 100% during austral spring (15 mm day^{-1} compared to observed 7–8 mm day^{-1}), and by 30% during austral fall (13 mm day^{-1} compared to observed 8–9 mm day^{-1}). The modeled precipitation shows distinct semiannual peaks in spring and fall, whereas the measured precipitation, especially that observed by rain gauges, is nearly flat from November to April (Fig. 1b). The dry season in July has 50% less precipitation than observed at its minimum (2 mm day^{-1} compared to an observed 4–5 mm day^{-1}). Hence, the seasonal range of precipitation in the western equatorial Amazon is twice of that observed. Figure 1 also suggests that GPCP data have a low bias compared to rain gauge observations during the austral fall rainy season, possibly because of its known tendency without use of the microwave emission channel to miss liquid (warm) precipitation over land, such as that found during the Tropical Rainfall Measurement Mission (TRMM) and Large-Scale Biosphere–Atmosphere wet season campaign (e.g., Rutledge et al. 2000; Rickenbach et al. 2000). ECMWF overestimates precipitation in the eastern Amazon by 50% during the austral spring dry season, but agrees with the observations in the western Amazon. Because wet seasons in the equatorial Amazon tend to peak in spring and/or fall instead of summer, our analyses use October and April, the times of the maximum insolation, to represent austral spring and fall seasons.

The spatial distributions of precipitation simulated by the CTR for January, April, July, and October are compared to those derived from the GPCP precipitation averaged over the period of 1986–97 (Fig. 2). The seasonal migration and broad spatial features of the precipitation in the equatorial Amazon appear to be adequately simulated in the CTR run although the model substantially overestimates the amount of rain-

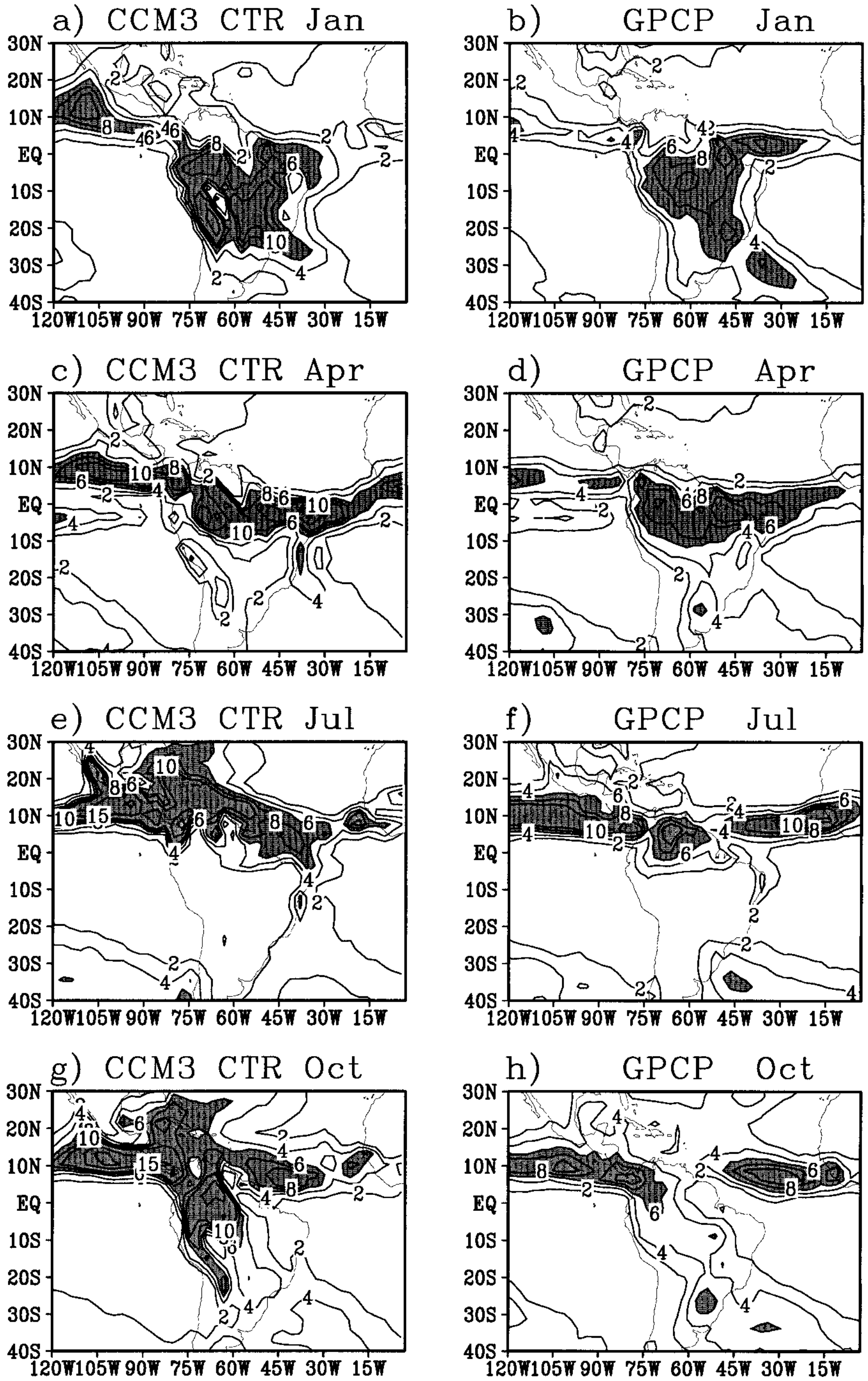

FIG. 2. Comparison of monthly precipitation between (a), (c), (e), (g) CCM3 control experiment and (b), (d), (f), (h) GPCP blended precipitation climatology (averaged over 1986–97) for (a), (b) Jan, (c), (d) Apr, (e), (f) Jul, and (g), (h) Oct. The contour interval is 2 mm day^{-1}. The areas where precipitation amount exceeds 6 mm day^{-1} are shaded.

fall in the western equatorial Amazon during austral spring and summer. The features most critical to this work, that is, the contrast of precipitation between the western and the eastern equatorial Amazon in austral spring (Oct), and the seasonal migration of Atlantic ITCZ, appear to be qualitatively well captured in the CTR run. The spatial structures of rainfall in austral summer (Jan) and fall (Apr) in the model also resemble those derived from the GPCP precipitation data, except that the dry tongue at 60°W in the equatorial

Amazon extends too far south in the model and subtropical South America is too dry in general. The worst discrepancy compared to observations is the extreme dryness of the model in the equatorial western Amazon in July (Fig. 2e). It is likely a result of the spurious shift of peak precipitation to the eastern equatorial Amazon and Caribbean Sea, as shown in Fig. 2f. However, such a spurious shift is minimal in austral spring (Oct). Hence, the distribution of rainfall in our experiments during the wet season should not be seriously affected by such defects in the control simulation.

The vertical structures of temperature, humidity, and horizontal winds in the CTR run are compared to radiosonde profiles and those assimilated in the ECMWF reanalyses. The daily profiles at 1200 UTC are averaged for each calendar month for the 10-yr CCM3 run, and for the period of 1983–93 for radiosonde and ECMWF reanalyses. At Belém (1.5°S, 49°W), near the east coast of equatorial South America, the modeled temperature profiles at 1200 UTC, that is 0720 local time, agree well with those of radiosondes and ECMWF reanalyses for all seasons (Figs. 3 and 4). The modeled humidity profiles also correspond closely to those of radiosondes below 800 mb, but underestimate humidity by 10%–40% in October (Fig. 3b). The ECMWF reanalyses at the same sampling time as the radiosonde profiles appear to systematically overestimate the humidity in the lower troposphere by 6%–12%. The vertical structure of zonal winds in CTR agrees generally with that given by the radiosondes except for being too easterly in the lower troposphere in October (Fig. 3c) and too westerly aloft during April (Fig. 4c). The former implies an excessive low-level inflow from the Atlantic Ocean in austral spring and also in winter (not shown). The meridional wind in CTR run show a much stronger vertical variation than that given by radiosonde, especially in October (Fig. 3d). The stronger vertical shear of meridional winds in CTR implies an excessive dynamic instability and mixing in the lower troposphere in austral spring. In April (Fig. 4d), a spurious peak of southerly wind appears at 800 mb and it may exaggerate the shear instability in the lower troposphere.

Figures 5 and 6 show that at Manaus in the central equatorial Amazon (2°S, 60°W, 1200 UTC, i.e., 0800 local time) the modeled lower troposphere is as warm as (Figs. 6a and 6b) or slightly warmer (up to 1–2 K, Fig. 5a) than observed, but drier by up to 10%–20% (Figs. 5b and 6b). The humidity of the lower troposphere in the ECMWF reanalyses, on the other hand, is about 10% higher than that observed by radiosondes. In October the modeled easterly wind, hence moisture transport, is too weak, probably contributing to the drier humidity at Manaus. In April, easterly zonal winds are about 50% stronger than observed below 400 mb, and too westerly above. The modeled meridional winds agree closely with those measured by radiosonde, except for a spurious southerly peak at 200 mb. Overall at Manaus, the agreement between CTR and radiosonde are comparable with that between the ECMWF reanalyses and observations.

How well CCM3 simulates the seasonal changes of large-scale atmospheric circulation is examined in terms of streamline and velocity potential at 200 mb in Figs. 7 and 8. It captures the anticyclonic flow of austral spring in the central Amazon centered at 10°S, but underestimates its magnitude (Figs. 7a and 7b). The velocity potentials in ECMWF and CCM3 agree as to locations of maximum divergence, but the orientation of the largest divergence (Figs. 7c and 7d), varies from NW–SE in ECMWF to NE–SW in CCM3. The Bolivian high weakens more in austral fall in CCM3 than in ECMWF (Figs. 8a and 8b). Although the streamline at 200 mb in ECMWF still shows a well-defined Bolivian high over the Altiplano Plateau in April, CCM3 only shows a weak anticyclonic flow confined to the north of 10°S. The velocity potential at 200 mb is consistent with this difference (Figs. 8c and 8d).

In summary, CCM3 can simulate the climatological seasonal cycle of precipitation in the equatorial Amazon, although the peaks are not reliably dated and in the west, too large in amplitude. The vertical temperature structures qualitatively agree with radiosonde profiles throughout all seasons, although humidity in the lower troposphere is significantly lower and the meridional winds show a much greater vertical variation than those observed. The large-scale upper-level flow and lower-level convergence are also reasonable, especially over land where seasonal changes of surface heat fluxes are more closely related to that of the insolation. The response of precipitation to the seasonal changes of large-scale atmospheric circulation and surface forcing appear to be physically and dynamically reasonable. The modeled distribution of precipitation is less reliable in July when CCM3 simulates a spurious center of precipitation over the Caribbean Sea, hence overestimating the lower-level divergence and subsidence over the equatorial Amazon. Evidently as a result of this shift, the humidity of the modeled lower troposphere is lower in the central equatorial Amazon than that observed.

4. How do SSTs affect the seasonality of Amazon rainfall?

a. *Without seasonal cycle of SSTs (ANN run)*

To determine the influence of seasonal variations of SSTs on Amazon rainfall, we first must isolate the contributions of land. Because the land surface responds to solar radiation almost instantly, precipitation dominated by land would follow the seasonality of solar radiation, and consequently would have a semiannual pattern with symmetry about the equator during the equinox seasons. Figure 9 shows the modeled annual cycles of precipitation averaged for the eastern and western equatorial

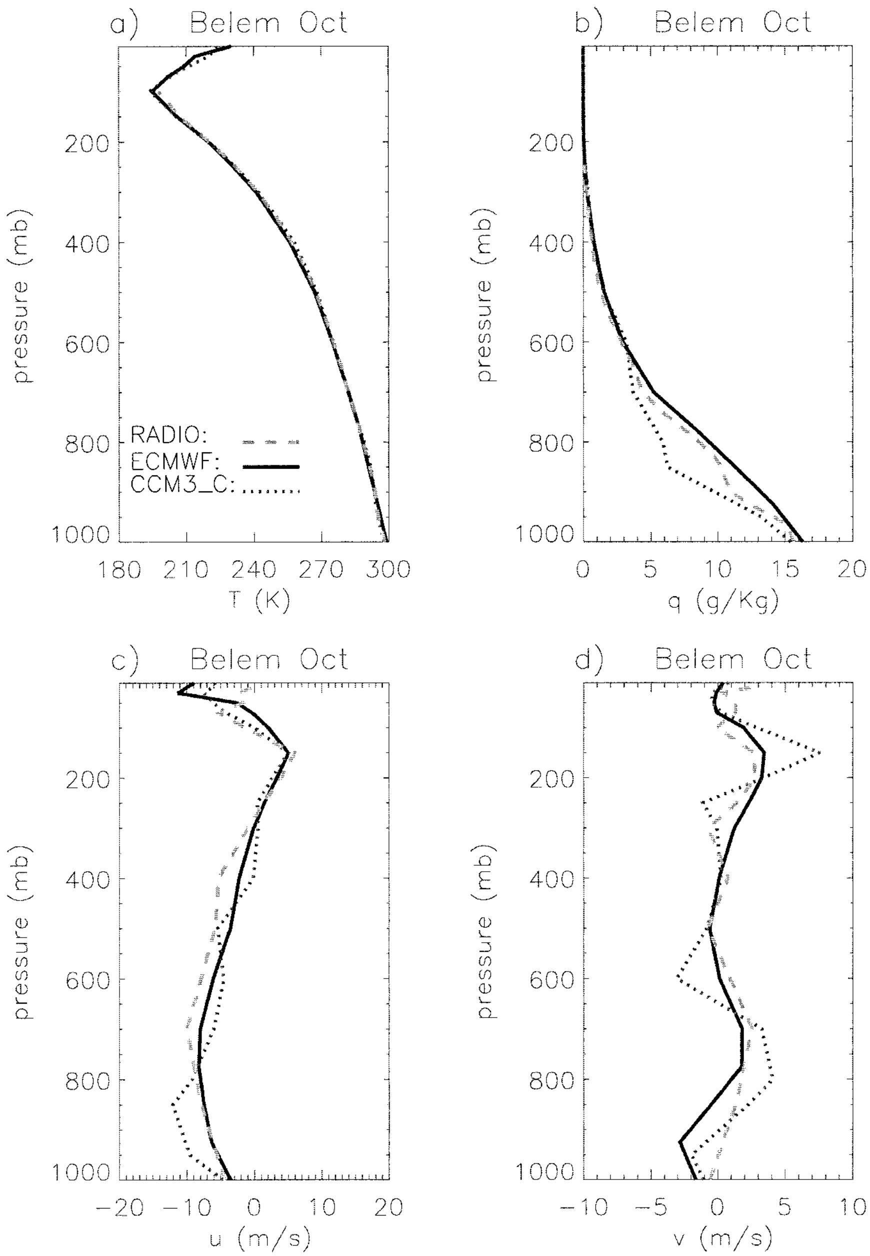

FIG. 3. Comparisons of the vertical profiles of (a) temperature, (b) humidity, (c) zonal, and (d) meridional winds between the CCM3 control experiment (dotted), radiosondes (dashed), and ECMWF reanalyses (solid) at Belém for Oct. The profiles of radiosondes and ECMWF reanalyses are obtained by averaging all the instantaneous values at each pressure level for each month for the period of 1987–93.

Amazon for the four cases. As expected, the seasonal cycle of precipitation in the ANN run without seasonality of the SSTs shows a semiannual pattern in the eastern Amazon whereas the CTR run shows an annual cycle peaking in austral fall.

Figure 10 shows the ANN spatial patterns of Amazon rainfall. In the solstice seasons (Figs. 10a and 10c), these spatial patterns of rainfall are very similar to those of CTR (Figs. 2a and 2e), suggesting that the seasonality of land heating largely control solstice precipitation. The patterns of prescribed annual mean SSTs in the eastern Pacific and Atlantic resemble more those of boreal than austral summer, keeping the eastern Pacific and Atlantic ITCZs to the north of the equator throughout the year. Precipitation at the equinoxes appears to be mostly influenced by the seasonality of SSTs over the tropical

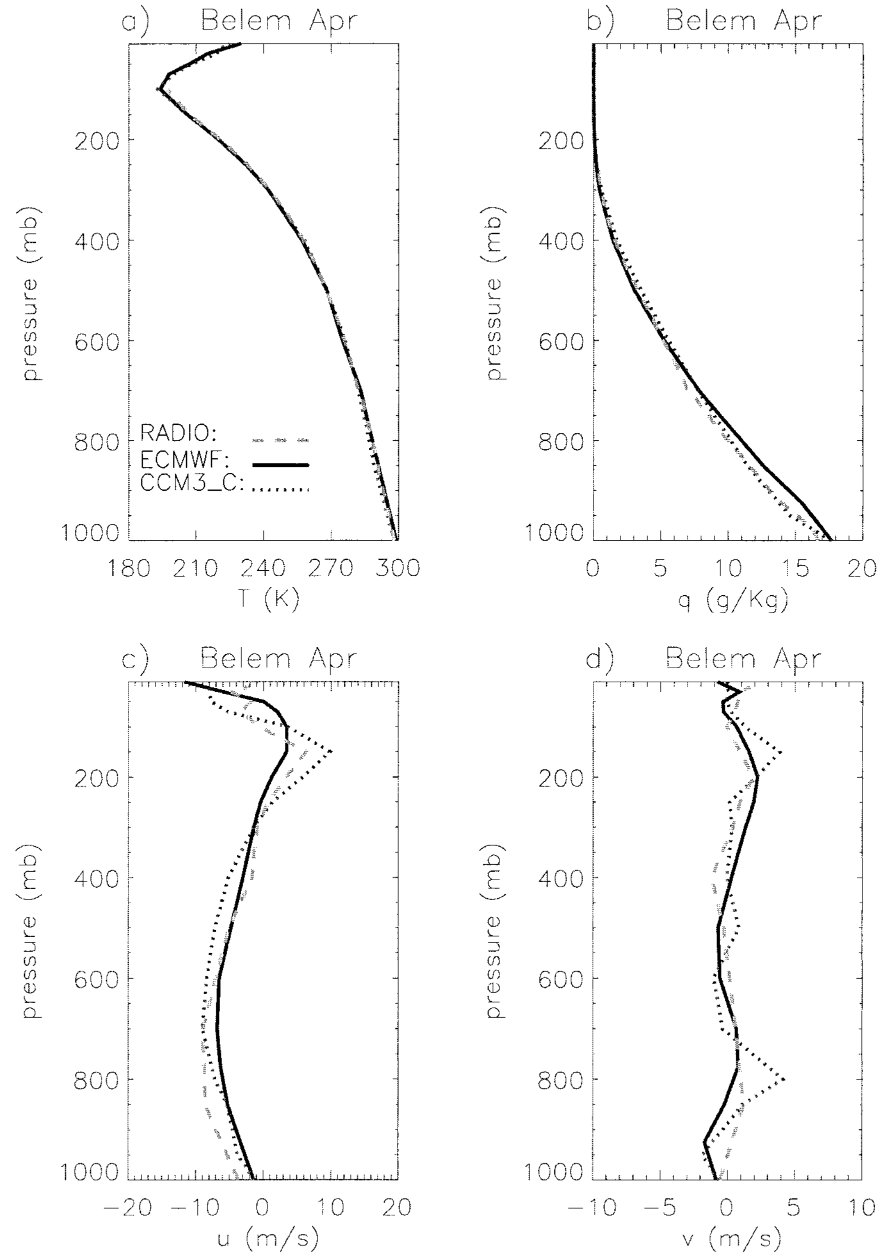

FIG. 4. As in Fig. 3 but for Apr.

oceans. The ANN precipitation in October (Fig. 10b) spreads across the entire equatorial Amazon, such that the eastern equatorial Amazon has much more rainfall than that in CTR (Fig. 2g). The Atlantic ITCZ, on the other hand, becomes weaker and shifts toward the equator and is confined to the western equatorial Atlantic (cf. Fig. 10b to Fig. 2g), suggesting that the seasonality of SSTs tends to draw precipitation away from the Amazon. The eastern Amazon in the ANN run in April is drier and Atlantic ITCZ is weaker than in CTR and the ITCZ is centered to the north of the equator (Fig. 10d), rather than to the south as in the CTR run (Fig. 2c). In both equinox seasons, the modeled rainfall in the western Amazon of the ANN run remains similar to that of the CTR run, suggesting that in the western Amazon the seasonality of the continent dominates that of the precipitation.

In short, the seasonality of the tropical SSTs influences Amazon rainfall weakly during the solstice seasons, but more strongly during the equinox seasons, and most strongly in austral spring over the eastern Amazon. Without the influence of tropical SSTs, precipitation

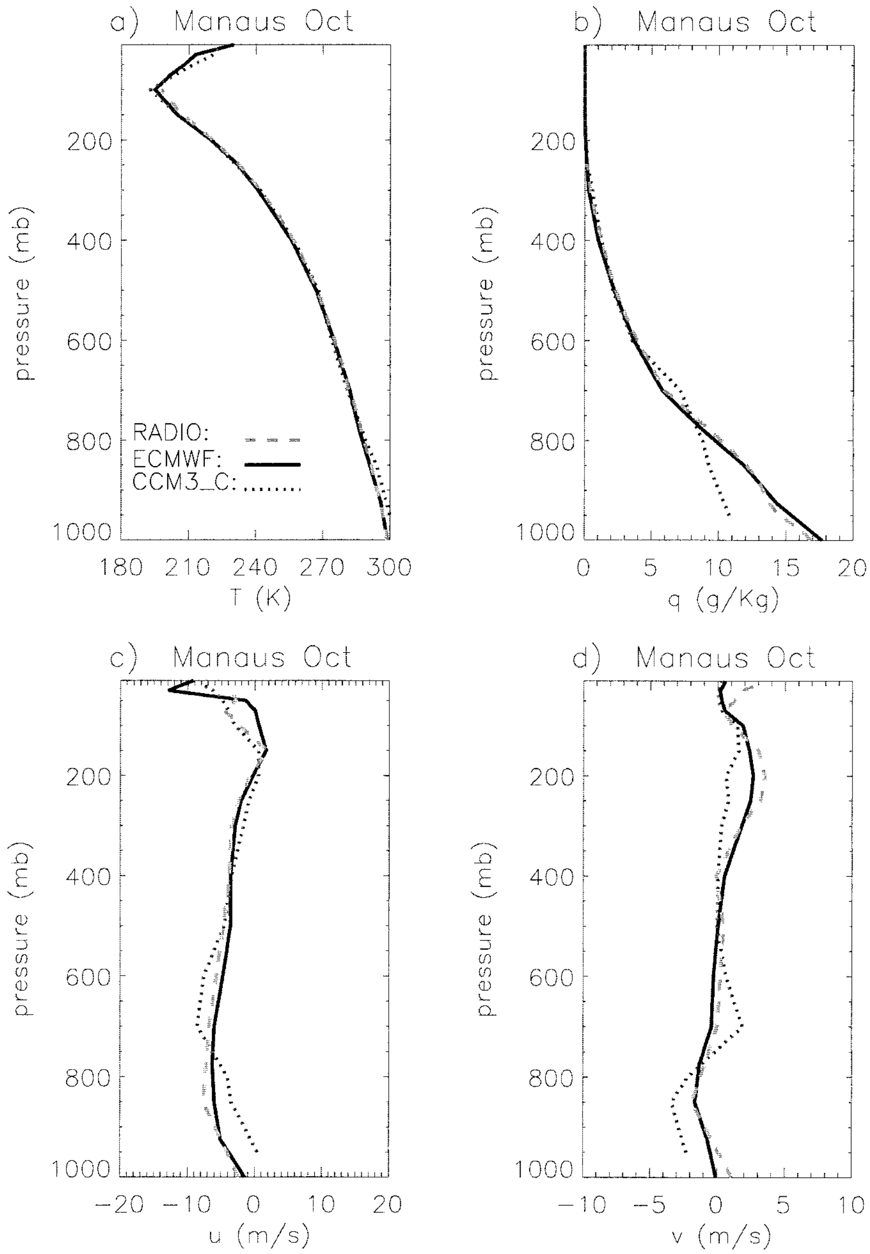

FIG. 5. As in Fig. 3, but at Manaus for Oct.

over the equatorial Amazon would have a semiannual seasonality following the insolation.

b. Tropical Atlantic

The results of the ATL run are compared with those of the ANN run to isolate how the seasonal cycle of Atlantic SSTs affects Amazon precipitation over the Amazon. The ATL and ANN runs differ only in the seasonal cycles of SSTs in the tropical Atlantic, as described in section 2. We will focus on the equinoxes because the influence of seasonal SSTs on Amazon rainfall during the solstices is relatively weak.

Figure 11 shows for October the seasonal departure of the SSTs in the Atlantic Ocean and the resulting difference in precipitation between ATL and ANN runs. Because the seasonal cycle of SSTs lags that of insolation, the ATL SSTs are still much warmer in the northern Atlantic and cooler in the southern Atlantic than their annual means (Fig. 11a). Consequently, the Atlantic ITCZ should remain in the North Atlantic, increasing oceanic precipitation to the north of the equator

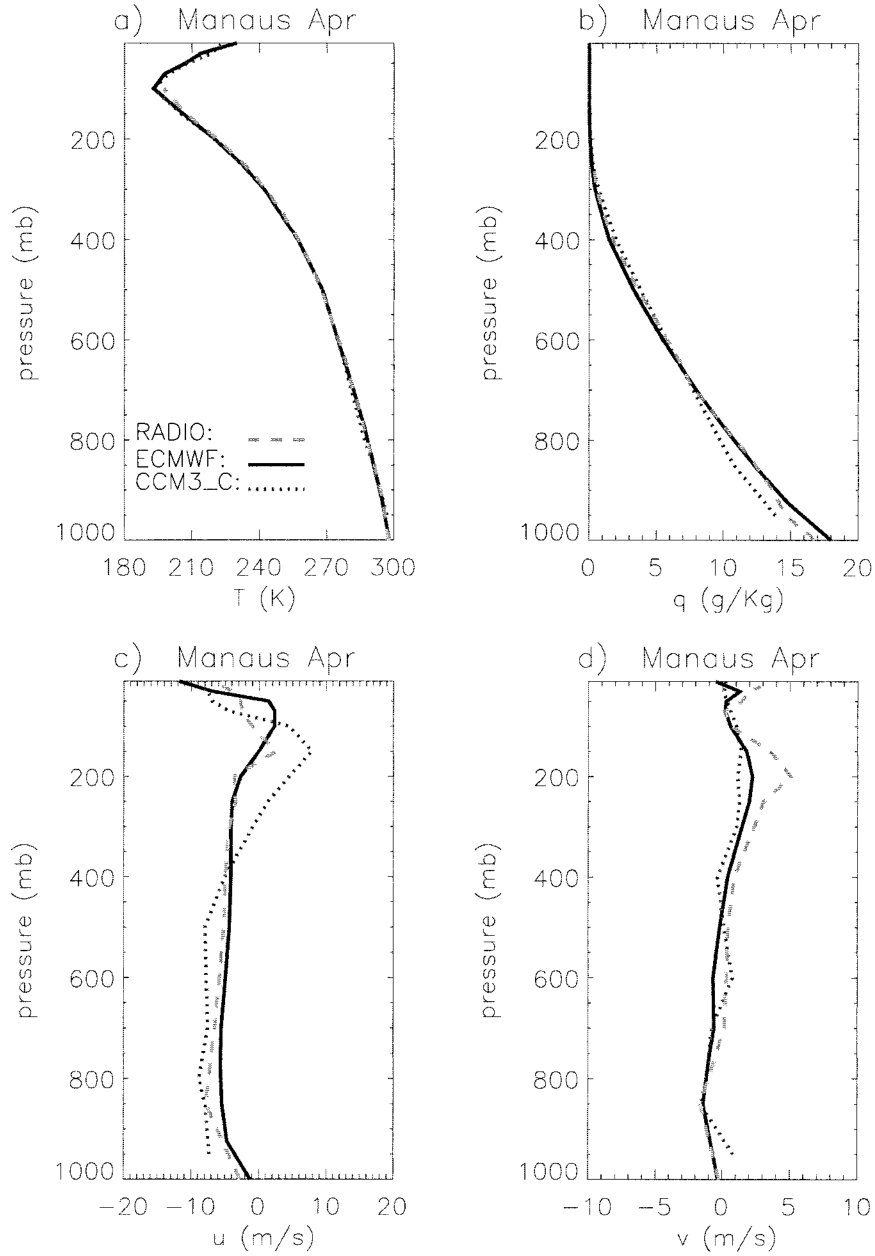

FIG. 6. As in Fig. 5, but for Apr.

and decreasing it to the south. The precipitation difference field in Fig. 11b supports this expectation. It is positive between 5° and 15°N over the Atlantic and Caribbean Sea and decreases to the south of 5°N in the Atlantic and eastern Amazon sector. Precipitation changes little in the western Amazon except for regions along the east slope of Andes, but is enhanced in Central America, north of the western Amazon. Subtropical precipitation increases over the continent, but decreases over the Atlantic Ocean, presumably a result of the SSTs in the South Atlantic being colder than their annual means. The eastern Pacific ITCZ appears to be displaced about 5° northward by the seasonal cycle of the Atlantic and Caribbean Sea SSTs, suggesting an Atlantic influence on the eastern Pacific ITCZ.

In April, the areas of increased precipitation are separated from those of reduced precipitation (Fig. 12b) by the sign of the departure of SSTs from their annual means (Fig. 12a), suggesting that the seasonal anomalies of precipitation over the Atlantic Ocean is directly related to those of SSTs. The increase of precipitation over the eastern Amazon appears as a westward extension of the enhanced Atlantic ITCZ. In contrast to October, precipitation also increases somewhat in the equatorial

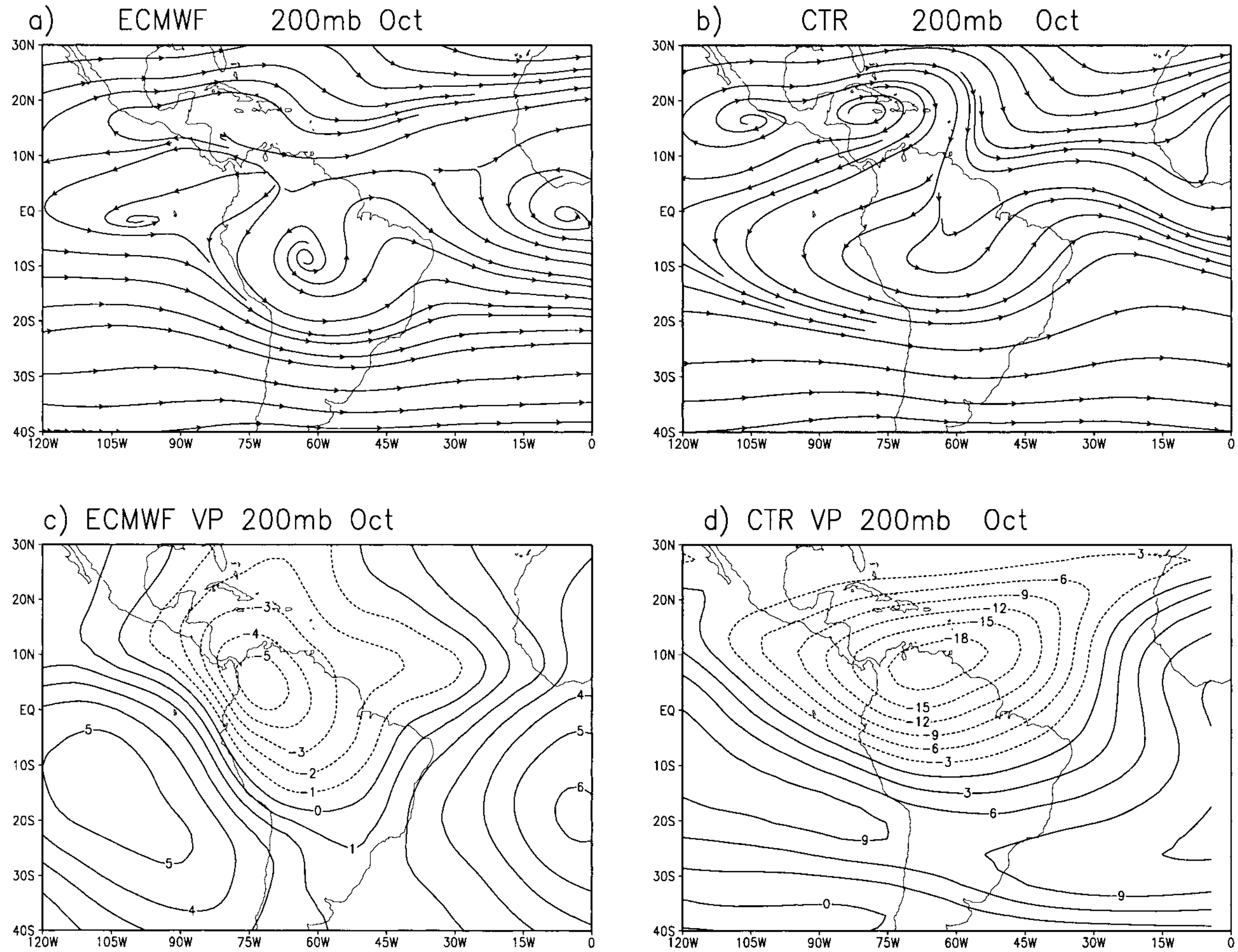

FIG. 7. Maps of streamline and velocity potential at 200 mb derived from ECMWF reanalyses and CCM3 control experiment for Oct averaged over the period of 1987–93. (a) Streamline derived from the ECMWF reanalyses. (b) As in (a) but from the CCM3 control experiment. (c) Velocity potential from ECMWF reanalyses. The unit is 10^6 m^2 s^{-1}. (d) As in (c) but from CCM3 control experiment.

western Amazon. The near-coastal end of the eastern Pacific ITCZ shifts equatorward, giving more rainfall between the equator and 10°N and less between 10° and 20°N.

c. Tropical Pacific

The PAC run is compared to ANN run in Figs. 13 and 14 to illustrate the influence of seasonality of tropical Pacific SSTs on Amazon rainfall. At both equinoxes, the dividing line between warmer and cooler seasonal anomalies tilts from 10°N in the eastern Pacific (80°–140°W) to 5° or 10°S in the central Pacific (160°E–180°; Figs. 13a and 14a). Hence, the spatial distribution of the seasonal departures of SSTs from their annual means in the tropical Pacific is more asymmetric relative to the equator than that in the Atlantic Ocean.

In October, the eastern Pacific ITCZ in the PAC run shifts northward by 5° from its location in the ANN run (Fig. 13b). SSTs south of 10°N in the eastern Pacific are cooler than their annual means (Fig. 13a), in the cold tongue region by as much as 2 K. Hence, the seasonality of the Pacific SSTs enhances the surface temperature contrast between the eastern Pacific and western Amazon. We might expect this to increase the gradient of mid- and upper-troposphere geopotential height, and consequently, rainfall in the western Amazon. However, Fig. 13b shows little change of precipitation in the western Amazon, but about a reduction of rainfall by 40%–60% in the eastern Amazon between the equator and 10°S. Hence, the influence of Pacific SSTs on Amazon rainfall cannot be simply explained by a thermal gradient between the eastern Pacific and the South American continent.

The eastern Pacific cold tongue is warmest in April and the South Pacific convergence zone is at its peak in terms of its eastward expansion. The north branch of the eastern Pacific ITCZ is weakest and closest to the equator (Fig. 14b). A south branch of the ITCZ appears between the equator and 5°S in the eastern Pacific. Consequently, precipitation increases between 5°N and 5°S, and decreases north of 5°N in the eastern Pacific. Com-

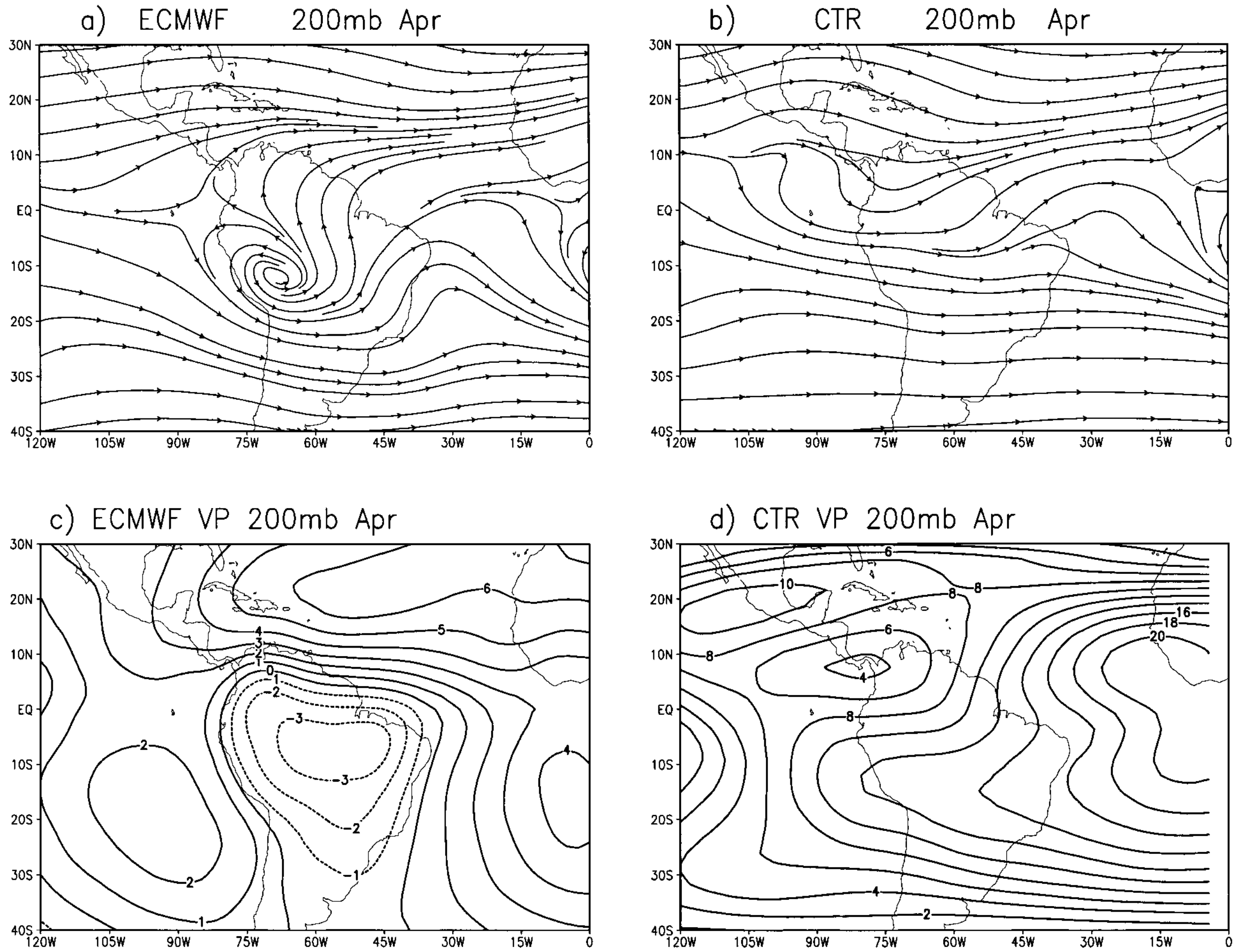

FIG. 8. As in Fig. 7 but for Apr.

pensational subsidence apparently suppresses precipitation over Central America and adjacent oceanic areas. Precipitation decreases over the eastern Amazon continent by 20%–40% on the equator coinciding with weakening of the Atlantic ITCZ. Rainfall increases in the western Amazon and along the east slope of the Andes across a very broad latitudinal range (10°N–30°S). These changes cannot be directly caused by the changes of land–ocean surface temperature contrast between the eastern Pacific cold tongue and the South American continent, since the southeastern Pacific is separated from the Amazon in the lower troposphere, and the resulting gradient of geopotential height between the Pacific and South American continent should decrease, rather than increase rainfall in the western Amazon.

5. The underlying mechanisms

a. Influence of the Atlantic Ocean

The response of precipitation to the ATL SST anomaly is largely a direct thermal cell, as supported by the upper-level pattern of divergence and convergence (Fig. 15b). The precipitation anomaly of the ITCZ has an outflow concentrated to its south by Hadley cell dynamics and to its west by a Rossby wave effect (Gill 1980). The low-level streamline pattern (Fig. 15a) has features similar to those described by Gill (1980). The trough over northern South America will amplify convergence north of the equator and divergence south of the equator through friction in the PBL, hence contributing to the shift of the precipitation anomaly westward onto northern South America and to the drying of the eastern Amazon. Hence, the direct circulation driven by seasonal migration of the tropical Atlantic SSTs shapes the seasonal pattern of rainfall at the equator in the eastern Amazon as it does interannual changes over the Nordeste (region of Brazil) (Moura and Shukla 1981).

The vertical-latitude cross section at 50°W (Fig. 16a) shows an enhanced area of rising motion occurring between 8° and 20°N over the Atlantic Ocean, a center of horizontal wind convergence below the 600-mb pressure level, and a center of divergence above the 300-mb pressure level. A subsidence to the south over the equatorial

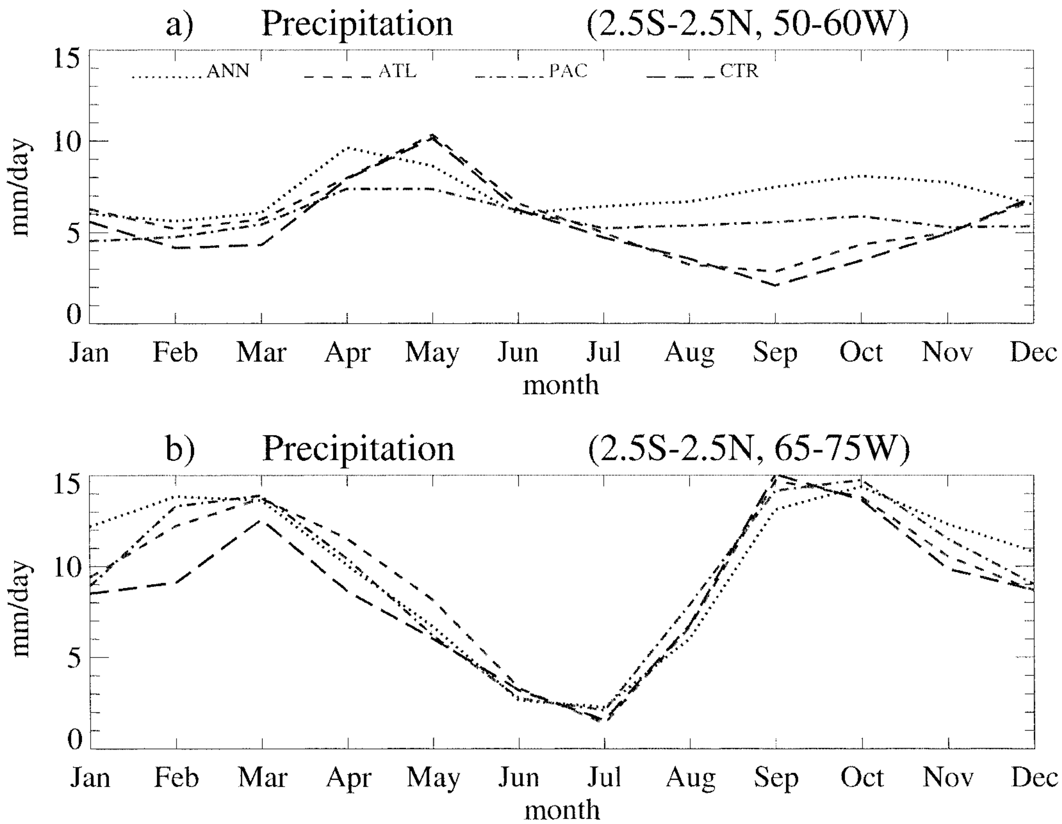

FIG. 9. Ensemble seasonal cycles of area averaged monthly precipitation amount (mm day^{-1}) over the (a) eastern and (b) western equatorial Amazon simulated by CCM3 CTR (long-dashed curve), ANN (dotted curve), ATL (dashed curve), and PAC (dot–dashed curve).

eastern Amazon compensates for this rising motion. However, over this subsidence region, divergence (solid contours) only appears at the surface over the Atlantic between the equator and 5°N. Over land, the enhanced subsidence leads to horizontal wind divergence, only over a layer from 600 to 850 mb, and not at the surface. A rising motion below 850 mb, presumably caused by increased solar heating of the land with decreased cloudiness, excludes subsidence from penetrating down to the surface. Evidently, the subsidence aloft induced by the Atlantic ITCZ suppresses the convection that otherwise would occur in response to the semiannual peak of surface heating in austral spring.

The zonal structure of the atmospheric response to the Atlantic SSTs in October is examined in the vertical-longitude cross section along 1.4°S (Fig. 16b). Strong subsidence and horizontal wind divergence in the lower troposphere are confined to the east of 55°W, corresponding to where precipitation is suppressed. In the western Amazon, the vertical velocity is essentially unchanged except for areas near 60°W, consistent with the unchanged precipitation in the western equatorial Amazon, although the meridional wind becomes more convergent near the surface especially along the east slope of the Andes.

Figure 17 explores how the circulation affects static and shear instability in October for the grid square containing Belém (1.5°S, 49°W). Averaged over the month and diurnally, the surface temperature in ATL at Belém exceeds that of ANN by only about 1 K. However, temperatures between 850 and 800 mb increase by about 2 K, implying a decrease of lapse rate and, consequently, a more stable stratification below 800 mb. Seasonality of Atlantic SSTs decreases the specific humidity by at least 2 g kg^{-1}. These changes increase the Convective Inhibition Energy (CINE; Williams and Renno 1993) by 41 J kg^{-1} in October or 27 J kg^{-1} averaged from September to December. This additional initial updraft velocity of up to 9 m s^{-1} required to overcome this extra CINE suppresses convection.

The meridional winds in the lower troposphere become more southerly, and above 600 mb more northerly, consistent with the anomalous low-level divergence and upper-level convergence in the equatorial eastern Amazon (see Fig. 16a). The zonal winds become more easterly in the lower troposphere and more westerly in the midtroposphere, such that zonal convergence weakens in the lower troposphere and divergence weakens aloft. Since transport is the main source of the moisture in that region (Marengo 1992; Rao et al. 1996; Brubaker

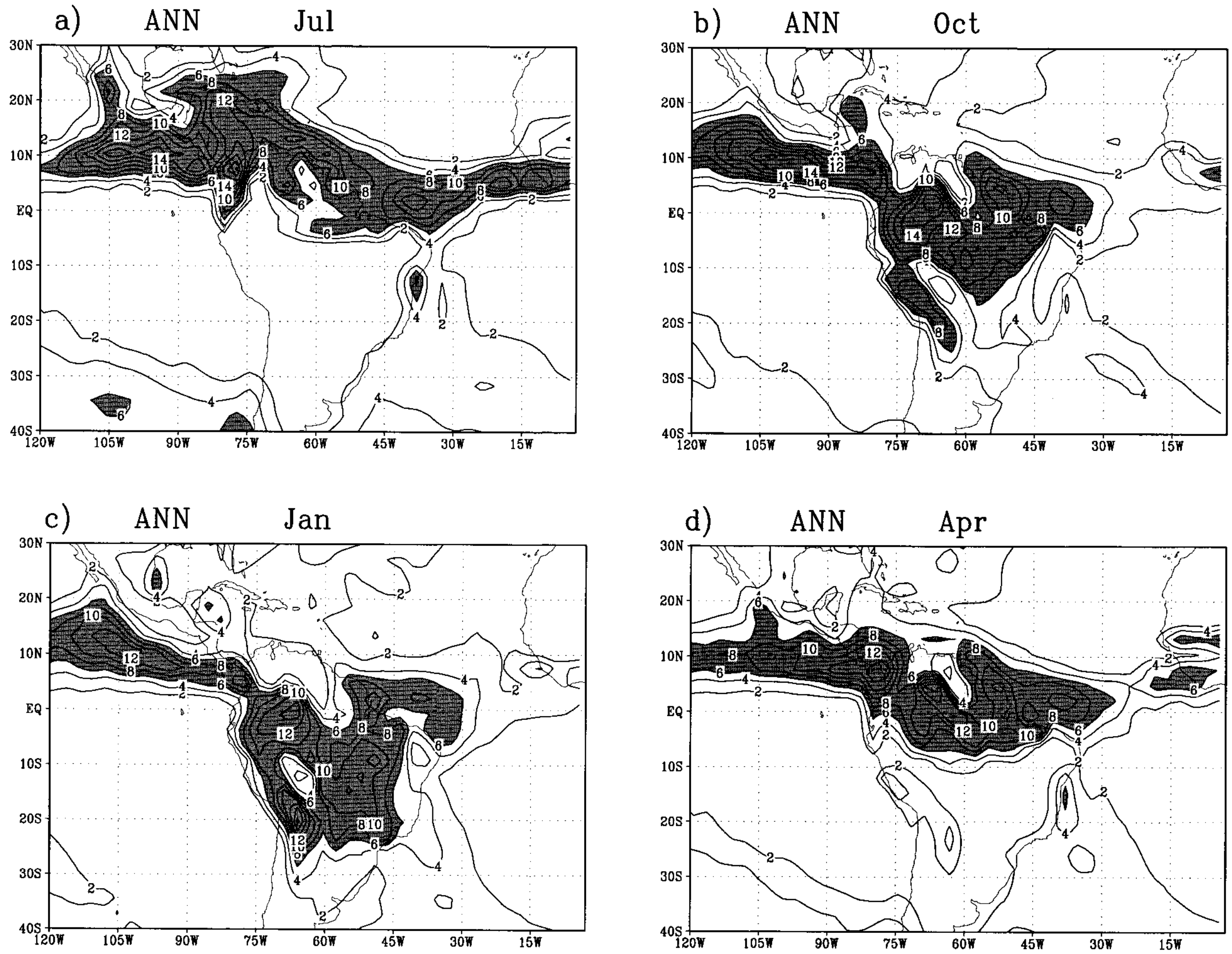

FIG. 10. Geographic distribution of precipitation (mm day^{-1}) in ANN run for (a) Jul, (b) Oct, (c) Jan, and (d) Apr.

et al. 1993), the weakened lower-tropospheric convergence contributes to the observed drier humidity. The shear of low-level winds, hence the shear instability needed for supporting the squall line type of convection (Silva Dias and Ferreira 1992) is also weaker (not shown) under the influence of seasonal departure of Atlantic SSTs in October from their annual means.

The results for April suggest a similar direct thermal circulation in response to the Amazon rainfall as in October, although with a different spatial pattern of precipitation anomaly. In summary, the differences between the ATL and ANN simulations show that the annual cycle of SSTs in the tropical Atlantic Ocean can significantly alter the spatial pattern of the precipitation at the equinox or from that determined by the seasonal cycle of continental heating in the Tropics. The direct thermal circulation in response to the Atlantic SST anomalies suppresses the wet season in the eastern equatorial Amazon during austral spring, evidently because the southward migration of the warmest SSTs and ITCZ in the Atlantic Ocean lag that of maximum solar radiation and thus clear-sky land surface heating. The location of the Atlantic ITCZ, at 10°N in austral spring, induces subsidence and meridional divergence of low-level wind over the equatorial eastern Amazon and Atlantic, stabilizing the lapse rate, reducing humidity within and above its boundary layer, and consequently inducing a statically and dynamically more stable large-scale environment. Hence, deep tropospheric convection and precipitation are suppressed. In austral fall, the SSTs anomalies are largest south of the equator. The cooler SST anomalies to the north enhance the meridional pressure gradient near the surface and promote subsidence north of 5°N. Rising motion and precipitation therefore are enhanced in the region of 5°N–15°S.

b. Influence of tropical Pacific

1) AUSTRAL SPRING

Pacific SSTs also generate wind anomalies that in turn modify precipitation over the Amazon. Wind anomalies are analyzed for 200 and 850 mb. Figure 18a shows the anomalies for October at 200 mb are westerly over the

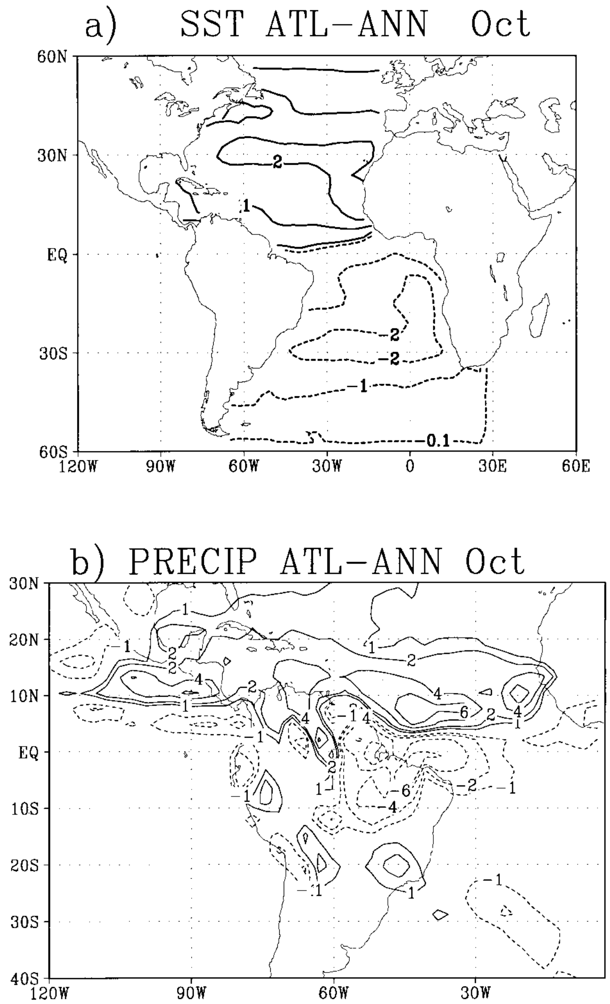

FIG. 11. Maps of the differences in (a) climatological SSTs and (b) precipitation between ATL and ANN for Oct. The contour interval in (a) is 1 K and in (b) is 2 mm day^{-1}. Solid contours indicate positive (warmer) values and dashed contours indicate negative (colder) values in both figures.

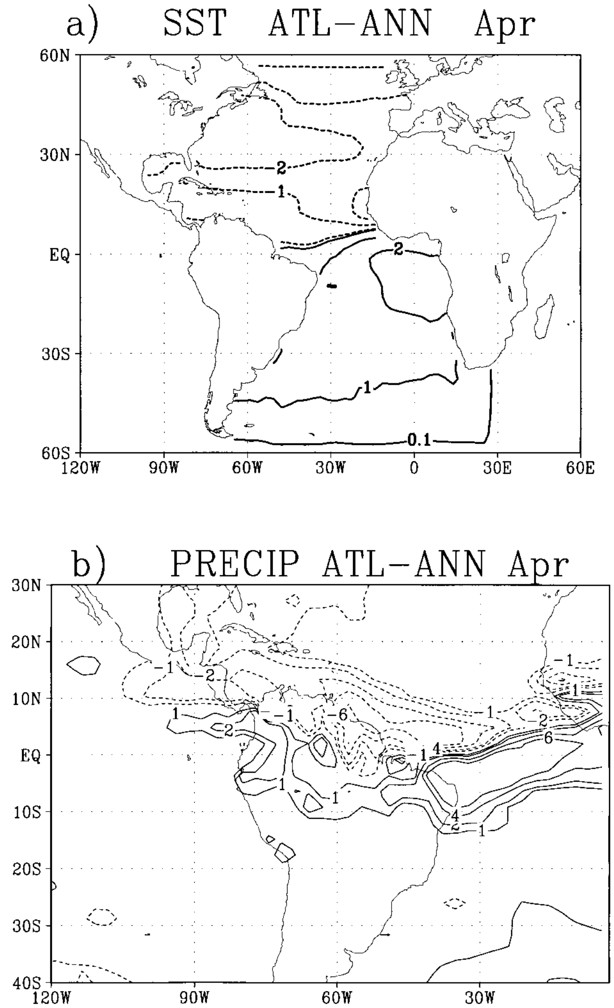

FIG. 12. As in Fig. 11 but for Apr.

northern and southern subtropical Atlantic and easterly over the equator. The consequent anticyclonic perturbation is especially strong over the subtropical eastern South America and western South Atlantic, the typical location of the the South Atlantic convergence zone (SACZ). The anomalies at 850 mb (Fig. 18b) are easterly over the Atlantic just north of the equator but become westerly in the Pacific with consequent convergence. The negative precipitation anomaly in the eastern Amazon (Fig. 13b) appears to be connected to the anticyclonic perturbation. The latter appears to be a response to the central Pacific SST anomalies. The low-level wind anomaly pattern also suggests that the negative precipitation anomaly is in part a response to the precipitation anomalies in the eastern Pacific through a direct thermal circulation.

How the response of large-scale circulation shown in Fig. 18 affects convective instability is examined through Figs. 17 and 19. Figure 17 shows for Belém that vertical profiles of temperature and humidity change little from ANN to PAC. Most noticeable is the temperature increase at 800 mb of 1 K, suggesting a strengthening of the inversion at the top of the PBL. Winds also change less than in ATL. Evidently, the seasonal cycle of SSTs in the Pacific influences only the free atmosphere above the PBL, and has little influence on the modeled vertical profiles of temperature, humidity, and winds, in contrast to the influence of the seasonal cycle of Atlantic SSTs.

The vertical cross section along 55°W (Fig. 19) shows that subsidence above 700 mb in PAC relative to ANN leads to horizontal wind divergence between 850 and 600 mb over the eastern Amazon between the equator and 15°S, with a southerly wind at the equator and a northerly wind at 10°S. This divergence in the low to midtroposphere suppresses deep convection in the eastern Amazon in spite of an increase in convergence and rising motion near the surface. The anomalous horizontal convergence and rising motion deepen over the sub-

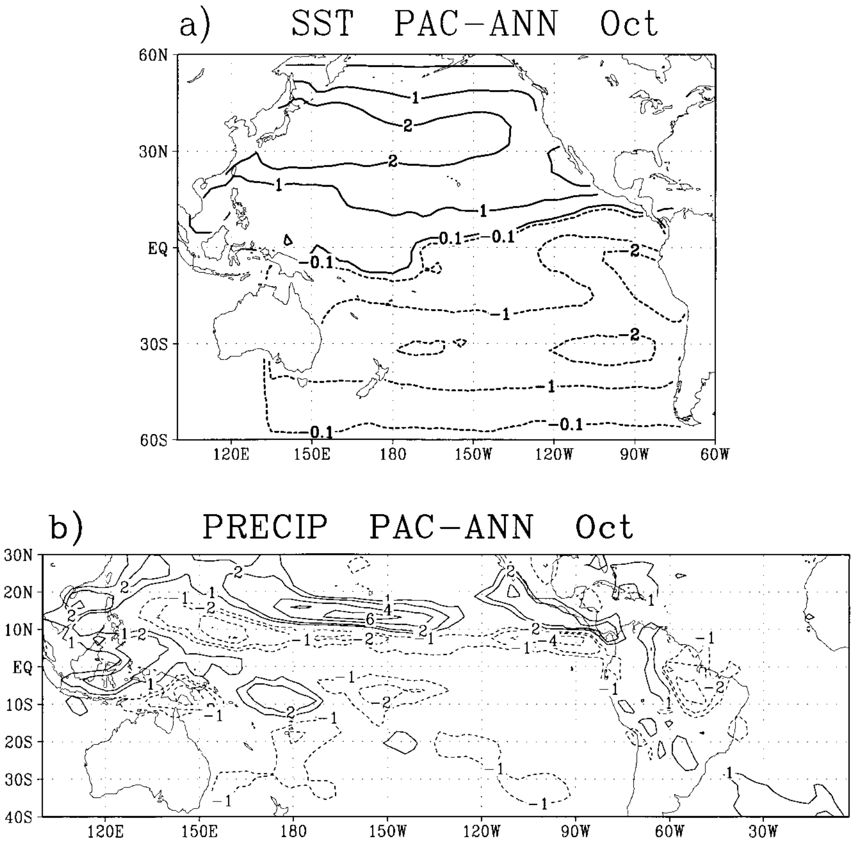

FIG. 13. As in Fig. 11, but for the differences between PAC and ANN runs.

tropical eastern South America continent (20°–30°S) in the PAC run.

Previous studies have suggested that either the combined effect of Amazon rainfall and the South Atlantic subtropical high (Cook 2000) or extratropical-to-tropical propagation of a Rossby wave can influence the SACZ (Kalnay et al. 1986; Liebmann et al. 1999; Robertson and Mechoso 2000). To identify the cause of the PAC anomalous upper-level anticyclonic flow over the SACZ in the austral spring, we plot the differential streamfunction at 200 mb and the wave activity flux (Karoly et al. 1989) in Fig. 20a. The contribution of the zonal mean flow to the streamfunction is removed to highlight the wave structure. The plot shows that a negative anomaly indicating upper-level anticyclonic flow centered on the east side of the South American continent in the subtropics is sandwiched between cyclonic flow anomalies to its northeast and southwest, respectively. This pattern is indicative of a wave train anomaly in the South Pacific and American sector, extending from the Tropics to the extratropics. The accompanying northeastward flux of wave activity from the extratropical southeastern Pacific to the SACZ, strengthens the upper-level anticyclonic flow associated with SACZ and the cyclonic flow to its north. The latter in turn can suppress precipitation in the eastern Amazon. The source for the wave activity appears to be the central tropical Pacific in the region of maximum precipitation response to the SST anomaly. However, the lack of applicability of the wave activity flux definition over the equator precludes making this conclusion definitively.

Hence, further clarification is sought with a linear barotropic model. The model is forced by a prescribed heating source with the 200-mb mean flow of October. We have tested various locations for the heating source based on the difference of the precipitation field between PAC and ANN run (Fig. 14b). A heating dipole in the tropical central Pacific (0°–20°N, 160°E–150°W), corresponding to the increased precipitation shown in Fig. 14b caused by the northward shift of Pacific ITCZ, generates a response resembling the streamfunction and wave activity flux differences between the PAC and ANN runs over South America and the south-central Pacific (Fig. 20b).

2) AUSTRAL FALL

Figure 21 compares the change in winds in April between PAC and ANN at 200 and 850 mb to determine the process that decreases precipitation over the eastern Amazon. At 200 mb, westerly anomalies appear over South America located to the east of the eastern and

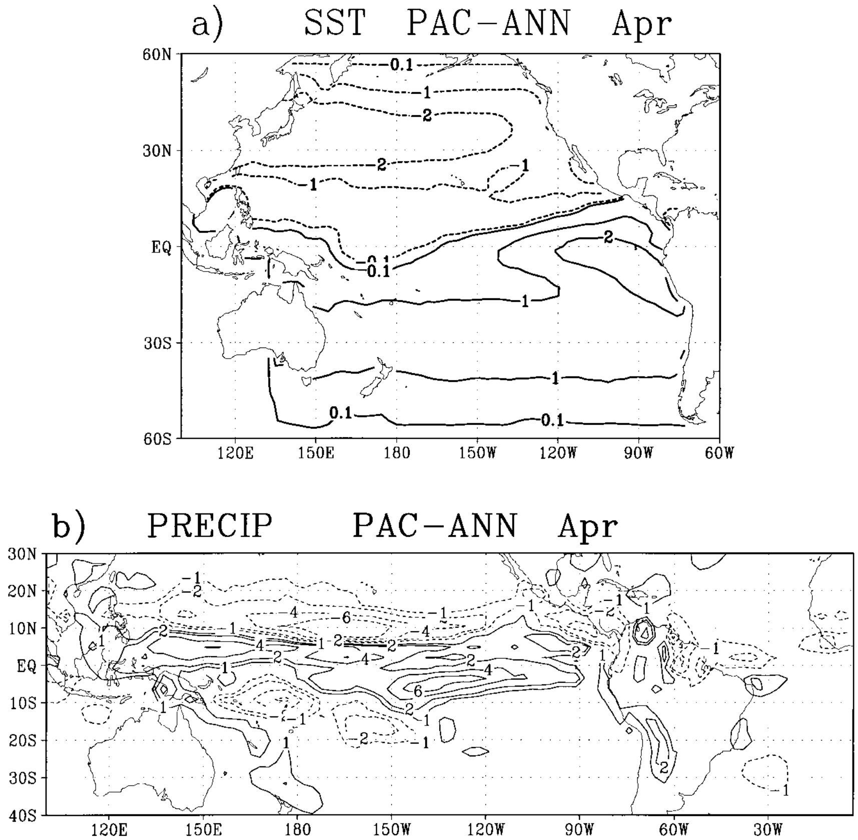

Fig. 14. As in Fig. 12, but for the differences between PAC and ANN run.

central equatorial Pacific precipitation anomalies (Fig. 13b). These anomalous westerlies shear cyclonically on either sides of the equator. The change of the flow at 850 mb east of the Pacific precipitation anomalies is reversed compared to that at 200 mb. The wind at 850 mb converges over the equatorial central Pacific (180°–120°W) and splits along the northwest and southwest flanks of the divergence region in the equatorial eastern Pacific (90°–120°E). The latter extends farther east to the South America continent. This pattern of wind divergence suggests a Walker cell response to the enhanced atmospheric heating in the central and eastern

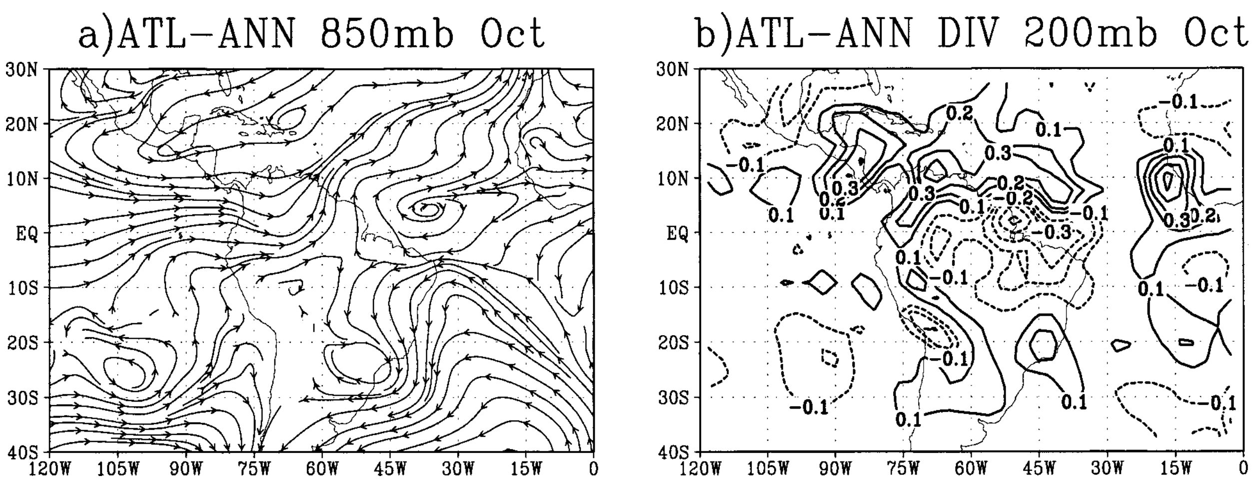

Fig. 15. Differences of monthly mean (a) streamline at 850 mb and (b) divergence at 200 mb simulated by ATL experiment from that of ANN experiment for Oct. The contour interval in (b) is 10^{-5} s^{-1}. Solid contours indicate positive deviations, and dashed contours indicate negative deviations.

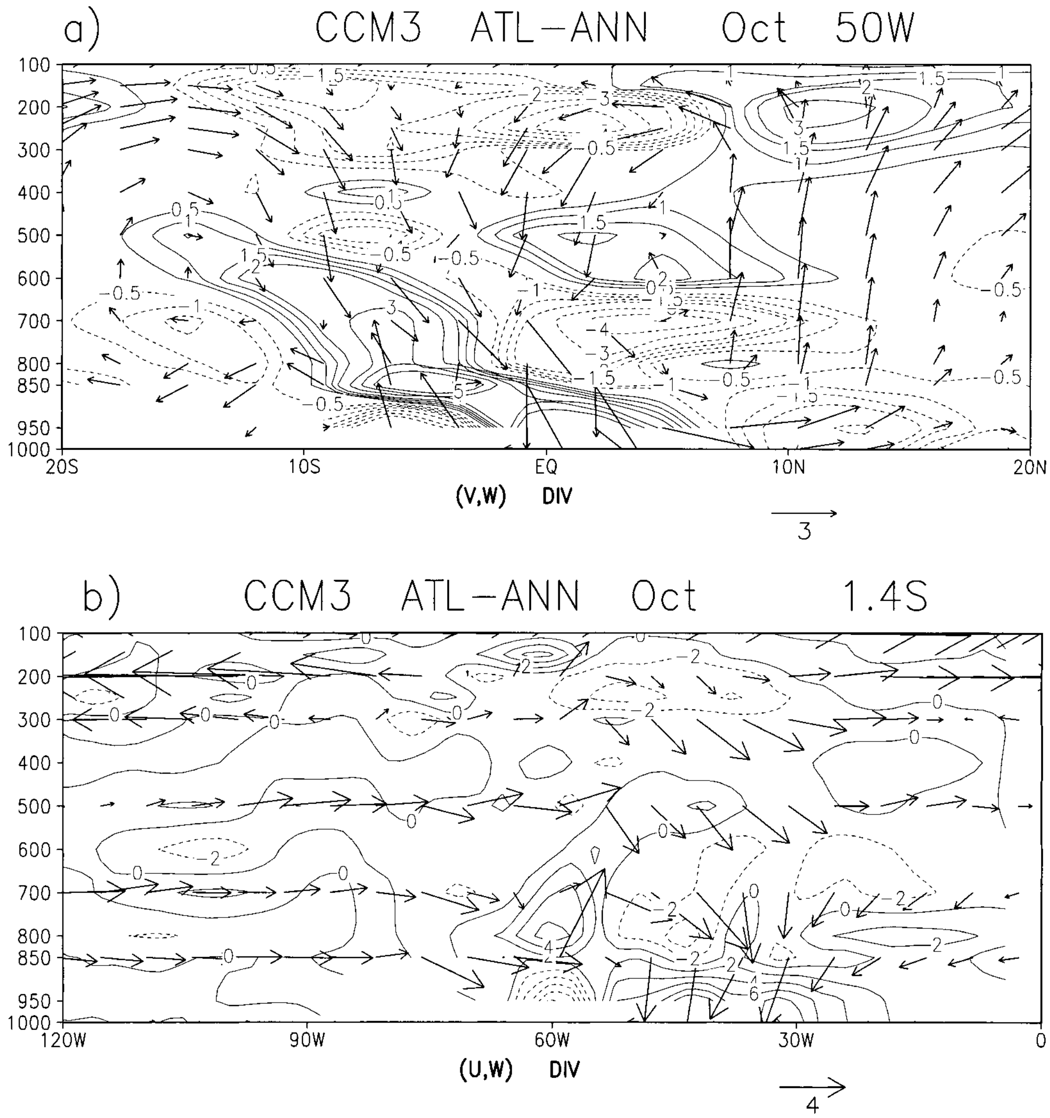

FIG. 16. (a) Differences in meridional and vertical winds (vectors), and horizontal wind divergence [$\partial u/\partial x + \partial v/\partial y$(contours)], between ATL and ANN experiment along the pressure-latitude cross section at 50°W for Oct. The length of the vector represents the magnitude of the wind and the arrow the direction of the wind. The scale is given near the lower-right corner of each diagram. The scale of the vertical winds is one-fiftieth of that of the horizontal winds. Solid contours indicate divergence and dashed contours convergence. (b) As in (a) but for the pressure–longitude cross section along 1.4°S. Vectors represent zonal and vertical winds. Contours represent horizontal wind divergence ($\partial \mathbf{u}/\partial \mathbf{x} + \partial \mathbf{v}/\partial \mathbf{y}$).

Pacific. The enhanced low-level divergence over the equatorial Amazon appears to be the sinking branch of the Walker cell response.

Although lower-level divergence is strengthened across the entire equatorial Amazon, precipitation only decreases in the east. Possibly topographic lifting of the enhanced lower-level northeasterly wind maintains precipitation along the east side of the Andes, despite the weakened lower-level convergence. In contrast to October, the absence of a wave train from the extratropical South Pacific to subtropical South America suggests that extratropical influences are probably unimportant for the decrease of precipitation in the equatorial eastern Amazon.

6. Discussion

a. Relative importance of land versus oceanic influence

The numerical experiments of Lenters and Cook (1995) have suggested that the South American continent is required for seasonal insolation to produce seasonality of precipitation over South America and the

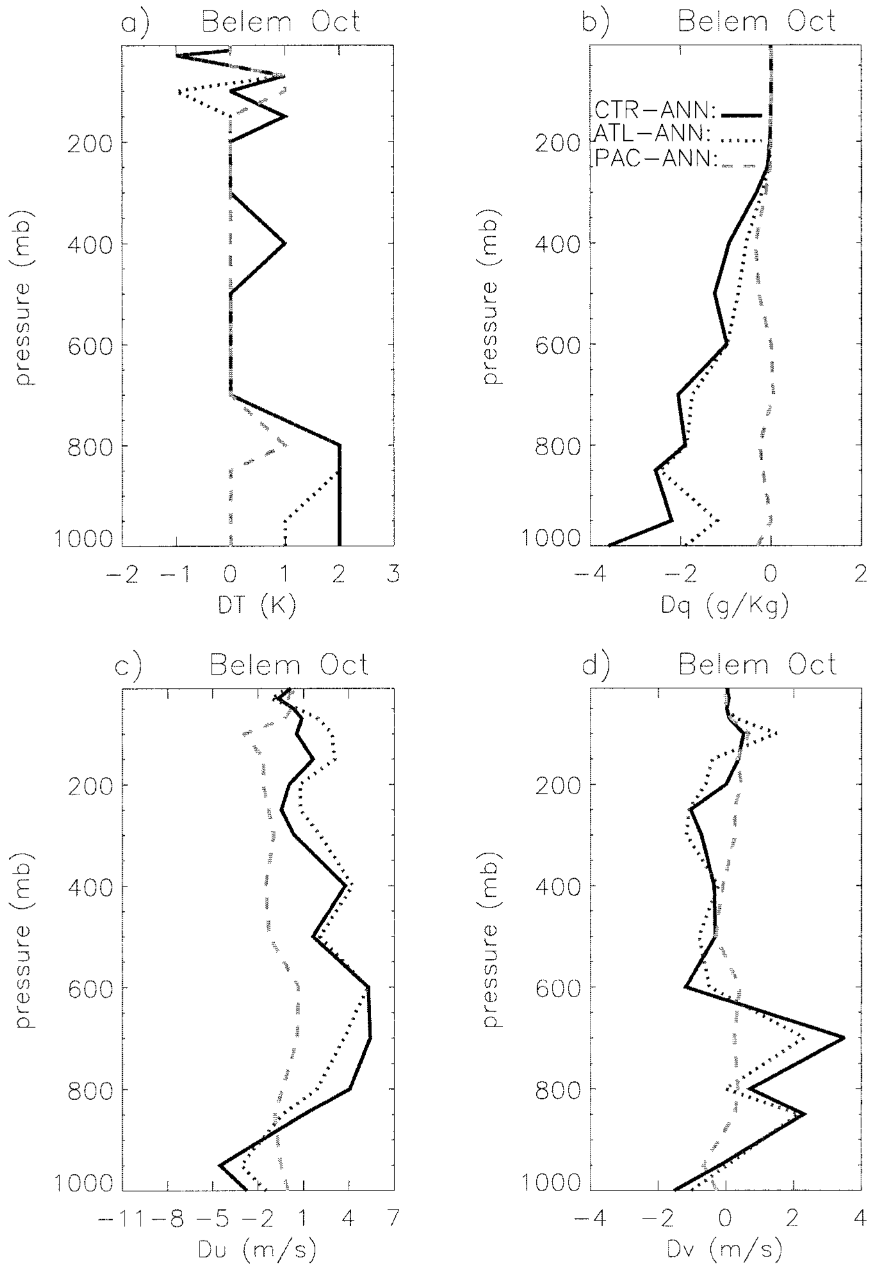

FIG. 17. The differences in vertical profiles of (a) temperature, (b) humidity, (c) zonal, and (d) meridional wind between CTR (solid), ATL (dotted), and PAC (dashed) experiments, respectively, and ANN experiments at Belém for Oct.

Bolivian high. Our comparison between ANN and CTR supports their conclusions for the western Amazon, the entire Amazon at the solstices, and the subtropical South American continent. However, in the eastern Amazon and at the equinoxes, the seasonal heating of the continent and seasonality of SSTs in the adjacent oceans appear to be equally important in determining the precipitation. Seasonal variations of SSTs of the tropical Pacific and Atlantic lag those of the continent and maximize at the equinoxes, at which time the atmospheric circulation over land, in transition between winter and summer, is most weakly affected by seasonality. The oceanic influence is more pronounced in the Tropics, where the seasonal change of land surface temperatures is weaker, than in the subtropics, where seasonality of the land surface is substantially stronger than that of the SSTs.

Our model simulation is consistent with observations that indicate a strong oceanic influence on precipitation in the eastern Amazon. Whether in the western Amazon,

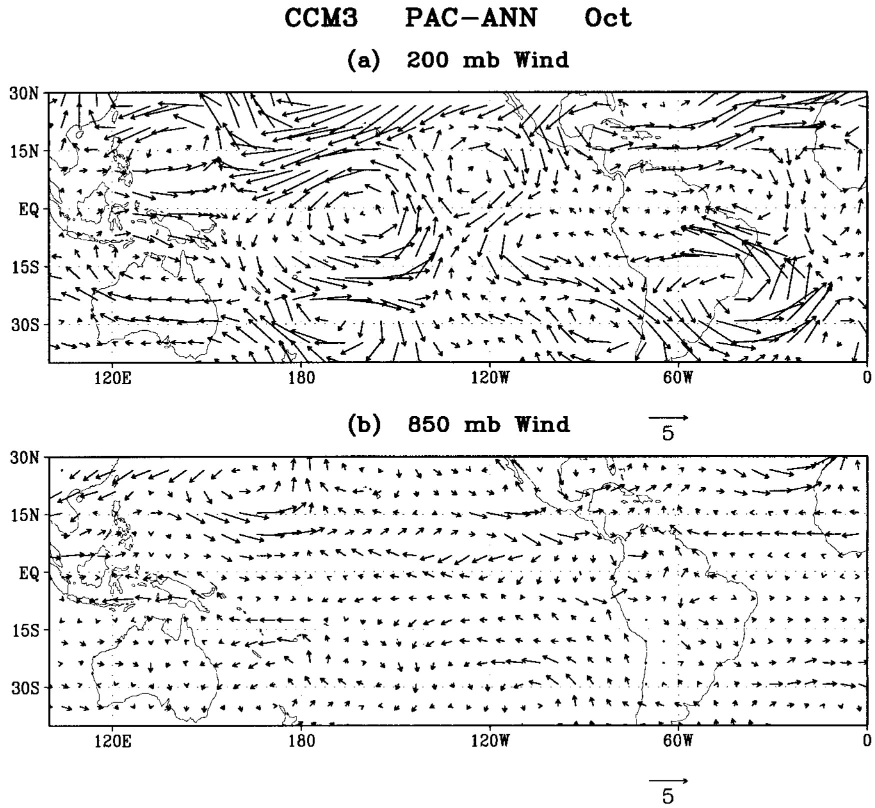

FIG. 18. Differences in monthly mean winds (m s^{-1}) at (a) 200 mb and (b) 850 mb between PAC and ANN experiments for Oct. The vector below the diagram on the right side indicates the scale of the wind difference for that diagram.

the oceanic influence on precipitation is indeed as weak as the model suggests needs further validation, a difficult task without reliable observations over the western Amazon. In addition, a higher model resolution may be needed to properly reproduce observations. Future observations that can be made with satellite systems such as TRMM may offer more reliable measurements of precipitation over the western Amazon.

b. Western Amazon versus eastern Amazon

Our numerical experiments show for the eastern equatorial Amazon that systematic responses of the upper-troposphere flow, the vertical velocity, and horizontal wind divergence above the PBL are related to the seasonal variations of the SSTs in the tropical Pacific and Atlantic. These responses consequently affect transport

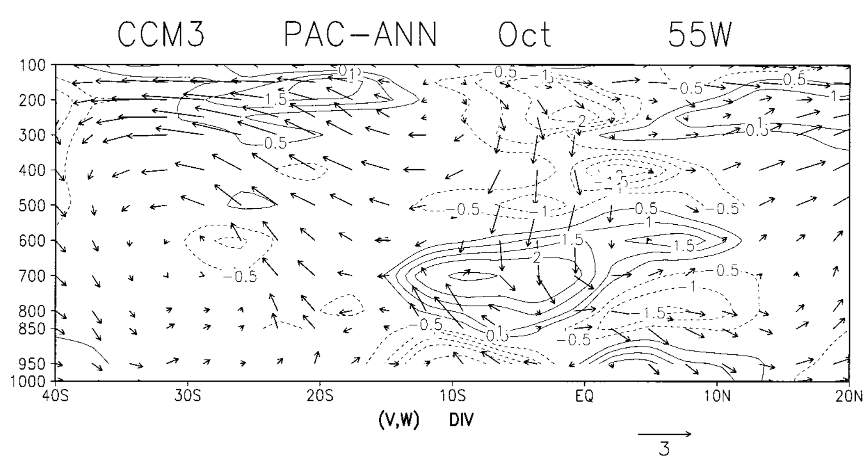

FIG. 19. As in Fig. 16a but for PAC minus ANN run along the 55°W for Oct.

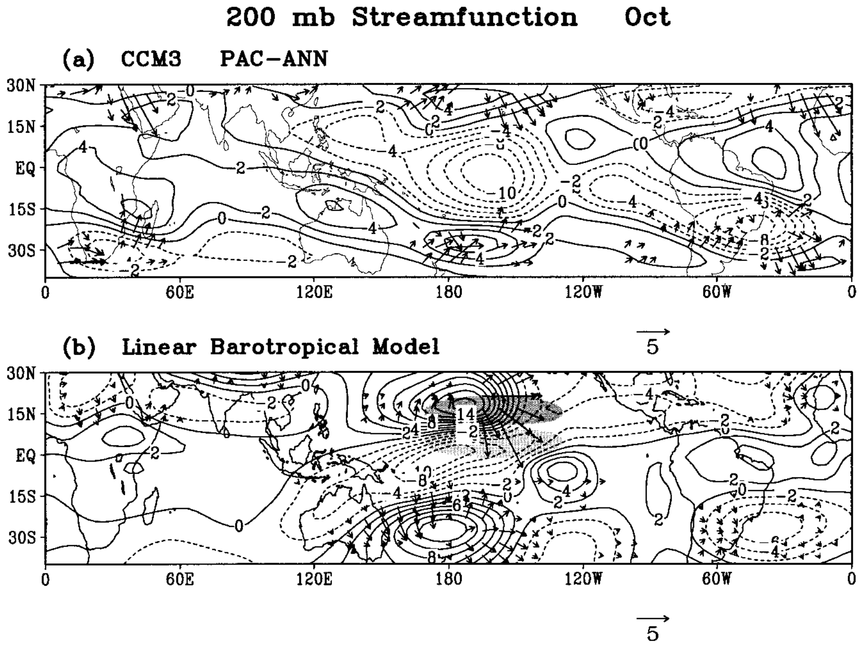

FIG. 20. (a) Differences in streamfunction at 200 mb between PAC and ANN run (contours) and associated wave activity flux (vectors) for Oct. (b) Streamfunction of the atmospheric response (contours) in the linear barotropic model to the heating (shaded areas) in the central Pacific and wave activity flux (vectors) for Oct. The contribution of the zonal mean flow to the streamfunction has been removed. Solid contours indicate counterclockwise flow, and dashed contours indicate clockwise flow. Wave activity index is not plotted within the region of 10°S–10°N. The darker shade indicates an upper-level divergence anomaly (a positive heating anomaly) and lighter shade indicates an upper-level convergence (a negative heating anomaly). The unit for contours is 10^6 m^2 s^{-1}.

of moisture from the Atlantic in the lower troposphere and the lapse rate above the PBL, and lead to a strong sensitivity of the precipitation in the eastern equatorial Amazon to the SSTs in the adjacent oceans. Over the western equatorial Amazon, the modeled seasonal change of precipitation is insensitive to the seasonality of the SSTs in any tropical oceans.

Why would the seasonal precipitation be more sensitive to SSTs over the eastern Amazon than over the western Amazon? The most likely factors explaining the difference are as follows:

1) The prevalent winds over the eastern Amazon originate from the Atlantic Ocean. Hence, changes of the Atlantic SSTs can easily affect the moist static energy of lower-tropospheric air, consequently convection in the eastern Amazon, as shown in our comparison between the ATL and ANN runs.
2) The atmospheric circulation over tropical South America is most influenced by heating anomalies in the tropical eastern Pacific, Caribbean Sea, and the western equatorial Atlantic. The strongest responses occur directly over these oceanic regions, rather than over the South American continent. The eastern Amazon is closer and more directly influenced by the responses centered over the tropical Atlantic than is the western Amazon.
3) Stronger topographic forcing and stronger effects of vegetation in the western Amazon may also contribute to the weaker sensitivity of the precipitation to oceanic influences.

c. The relative importance of the SSTs in tropical Atlantic and Pacific

Figure 9 shows that the seasonal cycle of the precipitation in the eastern Amazon in the CTR run can be largely reproduced by the ATL run, but not by the PAC and ANN runs. The seasonality of the Atlantic SSTs along with that of the continent evidently dominates the seasonal patterns of the Amazon rainfall. A direct thermal circulation carries Atlantic moisture to the Amazon. Without the influence of Atlantic SSTs, the annual peak in austral fall could be replaced by semiannual peaks in both spring and fall.

Pacific SSTs more weakly influence Amazon precipitation through a Walker cell response to the heating in the tropical central and eastern Pacific, and during austral spring, also through a response of a stationary Rossby wave train originating from the tropical central Pacific, and especially noticeable in the Southern Hemisphere. The influence of the Pacific SSTs is presumably further modified by the influences of the Atlantic SSTs

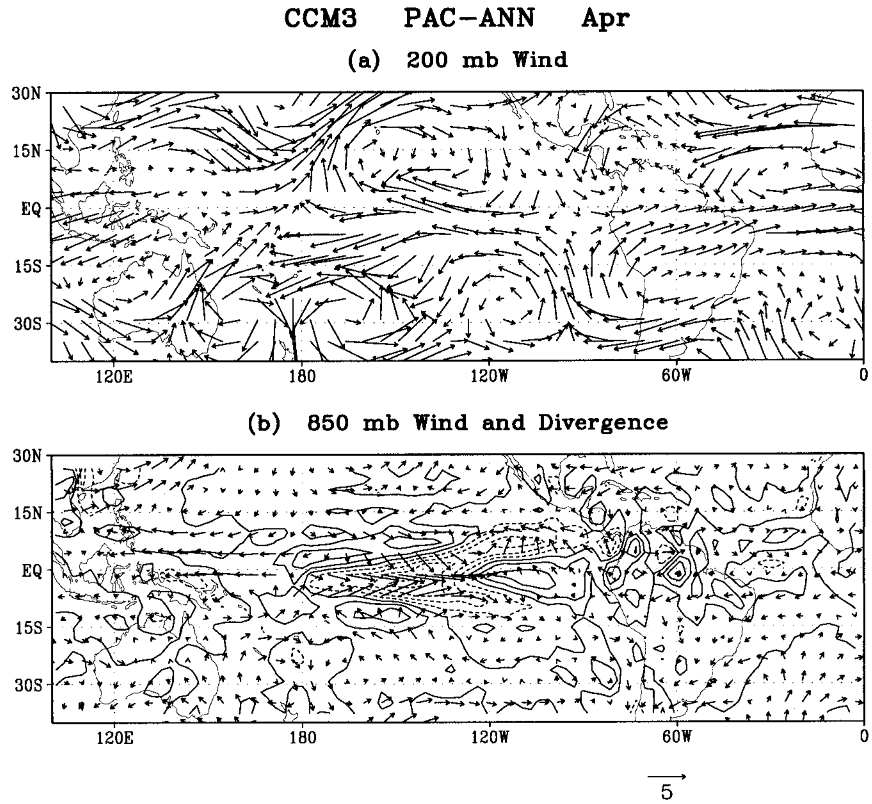

FIG. 21. As in Fig. 18, but for Apr and the addition of divergence/convergence at 850 mb. The solid contours in (b) indicate wind divergence at 850 mb, and the dashed contours represent convergence. The vector on the right side beneath diagram (b) indicates the scale for the wind field in both diagrams. The contour interval is 10^{-6} s^{-1}.

and Africa. Hence, the relationships between the Pacific SSTs and Amazon rainfall are complex with many factors involved.

In contrast to the seasonal variability, changes of the Pacific SSTs on interannual timescales, for example, ENSO, may contribute more to Amazon variability than those of the Atlantic because the SST changes in the latter are much weaker than those of ENSO.

d. Connection to observed interannual variability

The observed seasonal cycle of the atmospheric profiles of thermodynamic properties and their relationship to the large-scale atmospheric dynamic fields are consistent with a direct circulation response inferred from ATL. In particular, the austral spring rainfall in the equatorial eastern Amazon is suppressed by a strong inversion and dryness in the atmospheric PBL (Fu et al. 1999). Subsidence warms the atmosphere above the boundary layer and dries the boundary layer by its entrainment of the overlying stable air. These features are qualitatively captured, as shown in Figs. 15–17 in which changes of the precipitation and atmospheric circulation are solely caused by the seasonality of the Atlantic SSTs.

The propagation of the Rossby wave energy from the South Pacific to subtropical South America has been shown to enhance the SACZ (e.g., Kalnay et al. 1986; Liebmann et al. 1999; Robertson and Mechoso 2000), on the intraseasonal scale during summer. This teleconnection appears to simultaneously enhance the upper-level anticyclonic flow over the SACZ area and cyclonic flow over the eastern Amazon (Fig. 10 in Liebmann et al. 1999), similar to the responses of the upper-level flow to the austral spring distribution of the Pacific SSTs (Fig. 18) in our numerical experiments. Their summer results obtained from NCEP and ECMWF reanalyses support a possible influence of a Rossby wave train on precipitation in the eastern equatorial Amazon. However, further observational analyses are needed to clarify the existence of such a Rossby wave train response to seasonality of SSTs over the equatorial Pacific as suggested by the simulations.

Chiang et al. (2000) have observed that decadal variability of the Atlantic ITCZ and a zonally orientated dipole of precipitation at the equator over the tropical Atlantic are most sensitive to the anomalous heating dipole over the equatorial eastern Pacific during austral fall. Saravanan and Chang (2000) have analyzed CCM3 experiments that suggest interannual variability of the Atlantic ITCZ and precipitation in northeastern Brazil result from a circulation responding to the anomalous precipitation in the equatorial eastern Pacific. Their responses are similar to those in our experiments for seasonal variation.

7. Conclusions

We have performed four numerical experiments with different seasonal distributions of tropical SSTs using CCM3 coupled with BATS to test their influences on the seasonal distribution of precipitation over the equatorial Amazon. The control run (CTR) is forced by an observed climatological seasonal cycle of SSTs, the annual run (ANN) assumes fixed annual mean SSTs over global oceans. In the Atlantic (ATL) and Pacific (PAC) runs, SSTs vary seasonally either only in the tropical Atlantic or only in the tropical Pacific. The influences of SSTs globally and in each tropical ocean are examined by comparing CTR, ATL, and PAC runs to the ANN run.

The CTR shows a qualitative agreement with satellite-observed precipitation (GPCP), rain gauges, radiosonde profiles, and ECMWF reanalyses, especially during wet season. In particular, the contrast in duration of the wet season between the eastern and western Amazon is captured and seasonal changes of the vertical temperature stratification and humidity are reasonable. The model simulates a dry austral spring and a wet season of about three months in austral fall. However, a spurious shift of precipitation from the north-central Amazon to the Caribbean Sea during austral winter could reflect an inadequate response to the austral winter seasonal forcing, and may degrade the realism of our experiments. The modeled lower troposphere in the central equatorial Amazon is also systematically drier than observed by 20%.

The numerical simulations suggest these conclusions.

1) Seasonality of SSTs in the tropical Pacific and Atlantic has an important influence on precipitation in the eastern Amazon during the equinox seasons, and especially during austral spring. SSTs effect Amazon precipitation much less during the solstice seasons and in the western Amazon.
2) Seasonality of the Atlantic SSTs more strongly impacts Amazon rainfall than does that of the Pacific SSTs. Without the former, austral spring in the eastern equatorial Amazon would be a wet season, rather than the observed dry season. As a consequence of the lag of the southward seasonal migration of the Atlantic SSTs behind that of the insolation at that time, the Atlantic ITCZ centers itself near 10°N, instead of at the equator. Through a Hadley cell response, the ITCZ imposes subsidence and low-level anticyclonic flow over the eastern equatorial Amazon. The latter dries the air above the planetary boundary layer and reduces the low-level moisture convergence. Consequently, convection in the eastern Amazon is decreased despite the anomalous horizontal wind convergence and rising motion in the lower troposphere resulting from a stronger surface heating.
3) Seasonality of the SSTs in the tropical Pacific also tends to reduce precipitation in the eastern Amazon, both during spring and fall. In austral spring, the Pacific SSTs enhance the subsidence not only through zonal direct circulation, but also by a response of a stationary Rossby wave train ranging from the extratropical South Pacific to subtropical South America. This teleconnection strengthens the SACZ and the upper-level cyclonic flow to its north. The latter reduces precipitation in the eastern Amazon. The pattern of the response in the fall suggests that a Walker cell response to the anomalous precipitation in the central and eastern Pacific caused by seasonality of the Pacific SSTs reduces precipitation in the equatorial eastern Amazon. This mechanism has been invoked by Saravanan and Chang (2000) to explain the influence of ENSO on the Atlantic ITCZ during austral fall.

Acknowledgments. We are grateful to Dr. Thomas Dunne for kindly sharing his rain gauge data. We also thank Dr. Muhammad Shaikh and Ms. Wenhong Li for computational help; Drs. Andrea Hahmann, Michael Perdue, and Ronald Miller for constructive discussion, and two anonymous reviewers for their insightful comments. The radiosonde data and ECMWF reanalyses are provided by the NCAR Data Support Center. This work is supported by NOAA Global Office Pan American Climate Study (PACS) program, NASA Mission to Planet Earth New Investigator Program, and NSF Grant ATM 9727140.

REFERENCES

Aceituno, P., 1988: On the functioning of the Southern Oscillation in the South American sector. Part I: Surface climate. *Mon. Wea. Rev.,* **116,** 505–524.
Brubaker, K. L., D. Entekhabi, and P. S. Eagleson, 1993: Estimation of continental precipitation recycling. *J. Climate,* **6,** 1077–1089.
Buchmann, J., J. Paegle, L. Buja, and R. E. Dickinson, 1989: Further FGGE forecasts for Amazon rainfall. *Mon. Wea. Rev.,* **117,** 1093–1102.
Chiang, J. C. H., Y. Kushnir, and S. E. Zebiak, 2000: Interdecadal changes in eastern Pacific ITCZ variability and its influence on the Atlantic ITCZ. *Geophys. Res. Lett.,* **27,** 3687–3690.
Cook, K. H., 2000: Dynamics of the land-based convergence zones of the Southern Hemisphere. Preprints, *Sixth Int. Conf. on Southern Hemisphere Meteorology and Oceanography,* Santiago, Chile, Amer. Meteor. Soc., 356–357.
Dickinson, R. E., A. Henderson-Sellers, and P. J. Kennedy, 1993: Biosphere–Atmosphere Transfer Scheme (BATS) Version 1e as coupled to the NCAR Community Climate Model. NCAR Tech. Note NCAR/TN-387+STR, 72 pp.
Enfield, D. B., 1996: Relationship of inter-American rainfall to tropical Atlantic and Pacific SST variability. *Geophys. Res. Lett.,* **23,** 3305–3308.
Figueroa, S. N., and C. A. Nobre, 1990: Precipitation distribution

over central and western tropical South America. *Climanálise,* **5,** 36–45.

Fu, R., B. Zhu, and R. E. Dickinson, 1999: How do atmosphere and land surface influence seasonal changes of convection in the tropical Amazon? *J. Climate,* **12,** 1306–1321.

Gaffen, D., 1996: A digitized metadata set of global upper-air station histories. NOAA Tech. Memo. ERL, ARL-211, 38 pp.

Gandu, A. W., and P. L. Silva Dias, 1998: Impact of tropical heat sources on the South American tropospheric upper circulation and subsidence. *J. Geophys. Res.,* **103,** 60 001–60 015.

Gates, W. L., 1992: AMIP: The Atmospheric Modeling Intercomparison Project. *Bull. Amer. Meteor. Soc.,* **73,** 1962–1970.

Gibbs, J. R., 1979: Mechanism controlling world water chemistry. *Science,* **170,** 1088–1090.

Gill, A., 1980: Some simple solutions for heat-induced tropical circulation. *Quart. J. Roy. Meteor. Soc.,* **106,** 447–462.

Gutman, G. J., and W. Schwedtfeger, 1965: The role of latent and sensible heat for the development of a high-pressure system over the subtropical Andes in the summer. *Meteor. Rundsch.,* **18,** 69–76.

Hastenrath, S., and L. Heller, 1977: Dynamics of climatic hazards in northeast Brazil. *Quart. J. Roy. Meteor. Soc.,* **103,** 77–92.

Henry, A. J., 1922: The rainfall of Brazil. *Mon. Wea. Rev.,* **50,** 412–417.

Huffman, G. J., and Coauthors, 1997: The Global Precipitation Climatology Project (GPCP) combined precipitation dataset. *Bull. Amer. Meteor. Soc.,* **78,** 5–20.

Kalnay, E. K., C. Mo, and J. Paegle, 1986: Large-amplitude, short-scale stationary Rossby waves in the Southern Hemisphere: Observations and mechanistic experiments to determine their origin. *J. Atmos. Sci.,* **43,** 252–275.

Karoly, D. J., R. A. Plumb, and M. Ting, 1989: Examples of the horizontal propagation of quasi-stationary waves. *J. Atmos. Sci.,* **46,** 2802–2811.

Kiehl, J. T., J. J. Hack, G. B. Bonan, B. A. Boville, L. L. Williamson, and P. J. Rasch, 1998: The National Center for Atmospheric Research Community Climate Model: CCM3. *J. Climate,* **11,** 1131–1149.

Lau, N. C., and M. J. Nath, 1994: A modeling study of the relative roles of tropical and extratropical SST anomalies in the variability of the global atmosphere–ocean system. *J. Climate,* **7,** 1184–1207.

Lenters, J. D., and K. H. Cook, 1995: Simulation and diagnosis of the regional summertime precipitation climatology of South America. *J. Climate,* **8,** 2988–3005.

——, and ——, 1997: On the origin of the Bolivian high and related circulation features of the South America climate. *J. Atmos. Sci.,* **54,** 656–677.

Liebmann, B., and J. A. Marengo, 2001: Interannual variability of the rainy season and rainfall in the Brazilian Amazon basin. *J. Climate,* in press.

——, G. N. Kiladis, J. A. Marengo, T. Ambrizzi, and J. D. Glick, 1999: Submonthly convective variability over South America and the South Atlantic convergence zone. *J. Climate,* **12,** 1877–1891.

Marengo, A. J., 1992: Interannual variability of surface climate in the Amazon basin. *Int. J. Climatol.,* **12,** 853–863.

——, B. Liebmann, V. E. Kousky, N. P. Filizola, and I. C. Wainer, 2001: Onset and end of the rainy season in the Brazilian Amazon Basin. *J. Climate,* **14,** 833–852.

Moura, A. D., and J. Shukla, 1981: On the dynamics of droughts in northeast Brazil: Observations, theory and numerical experiments with a general circulation model. *J. Atmos. Sci.,* **38,** 2653–2675.

Namias, J., 1972: Influence of Northern Hemisphere general circulation on drought in northeast Brazil. *Tellus,* **XXIV,** 336–342.

Navon, I. M., and D. M. Legler, 1987: Conjugate-gradient methods for large-scale minimization in meteorology. *Mon. Wea. Rev.,* **115,** 1479–1502.

Nepstad, D. C., and Coauthors, 1999: Large-scale impoverishment of Amazonian forests by logging and fire. *Nature,* **398,** 505–508.

Nobre, P., and J. Shukla, 1996: Variations of sea surface temperature, wind stress and rainfall over the tropical Atlantic and South America. *J. Climate,* **9,** 2464–2479.

Rao, G. V., and S. Erdogan, 1989: The atmospheric heat source over the Bolivan Plateau for a mean January. *Bound.-Layer Meteor.,* **46,** 13–33.

Rao, V. B., I. Cavalcanti, and K. Hada, 1996: Annual variations of rainfall over Brazil and water vapor characteristics of South America. *J. Geophys. Res.,* **101,** 36 350–36 551.

Rickenbach, T. M., R. N. Ferreira, J. B. Halverson, and R. Cifelli, 2000: Evolution of mesoscale convective systems in contrasting large scale regimes from radar and infrared satellite data during the TRMM-LBA field campaign in Rondônia, Brazil. Preprints, *24th Conf. on Hurricanes and Tropical Meteorology,* Fort Lauderdale, FL, Amer. Meteor. Soc., 139–140.

Robertson, A. W., and C. R. Mechoso, 2000: Interannual and interdecadal variability of the South Atlantic convergence zone. *Mon. Wea. Rev.,* **128,** 2947–2957.

Rutledge, S. A., W. A. Petersen, R. C. Cifelli, and L. D. Carey, 2000: Early results from TRMM-LBA: Kinematic and microphysical characteristics of convection in distinct meteorological regimes. Preprints, *24th Conf. on Hurricanes and Tropical Meteorology,* Fort Lauderdale, FL, Amer. Meteor. Soc., 137–138.

Salati, E., A. Dall'Olio, J. Gat, and E. Matsui, 1979: Recycling of water in Amazon Basin: An isoptope study. *Water Resour. Res.,* **15,** 1250–1258.

Saravanan, R., and P. Chang, 2000: Interaction between tropical Atlantic variability and El Niño–Southern Oscillation. *J. Climate,* **13,** 2177–2194.

Silva Dias, M. A. F., and R. N. Ferreira, 1992: Application of a linear spectral model to the study of Amazonian squall lines during GTE/ABLE-2b. *J. Geophys. Res.,* **97,** 405–419.

Ting, M., 1996: Steady linear response to tropical heating in barotropic and baroclinic models. *J. Atmos. Sci.,* **53,** 1698–1709.

Weare, B. C., 1977: Empirical orthogonal function analysis of Atlantic Ocean surface temperature. *Quart. J. Roy. Meteor. Soc.,* **103,** 467–478.

Williams, E., and N. Renno, 1993: An analysis of the conditional instability of the tropical atmosphere. *Mon. Wea. Rev.,* **121,** 21–36.

Zebiak, S. E., 1993: Air–sea interaction in the equatorial Atlantic region. *J. Climate,* **6,** 1567–1586.